



Pacific Northwest
NATIONAL LABORATORY

Proudly Operated by Battelle Since 1965

Scale-Dependent Solute Dispersion in Variably Saturated Porous Media

March 2016

ML Rockhold
ZF Zhang
Y-J Bott

DISCLAIMER

This report was prepared as an account of work sponsored by an agency of the United States Government. Neither the United States Government nor any agency thereof, nor Battelle Memorial Institute, nor any of their employees, makes **any warranty, express or implied, or assumes any legal liability or responsibility for the accuracy, completeness, or usefulness of any information, apparatus, product, or process disclosed, or represents that its use would not infringe privately owned rights.** Reference herein to any specific commercial product, process, or service by trade name, trademark, manufacturer, or otherwise does not necessarily constitute or imply its endorsement, recommendation, or favoring by the United States Government or any agency thereof, or Battelle Memorial Institute. The views and opinions of authors expressed herein do not necessarily state or reflect those of the United States Government or any agency thereof.

PACIFIC NORTHWEST NATIONAL LABORATORY
operated by
BATTELLE
for the
UNITED STATES DEPARTMENT OF ENERGY
under Contract DE-AC05-76RL01830

Printed in the United States of America

Available to DOE and DOE contractors from the
Office of Scientific and Technical Information,
P.O. Box 62, Oak Ridge, TN 37831-0062;
ph: (865) 576-8401
fax: (865) 576-5728
email: reports@adonis.osti.gov

Available to the public from the National Technical Information Service
5301 Shawnee Rd., Alexandria, VA 22312
ph: (800) 553-NTIS (6847)
email: orders@ntis.gov <<http://www.ntis.gov/about/form.aspx>>
Online ordering: <http://www.ntis.gov>



This document was printed on recycled paper.

(8/2010)

Scale-Dependent Solute Dispersion in Variably Saturated Porous Media

ML Rockhold
ZF Zhang
Y-J Bott

March 2016

Prepared for
the U.S. Department of Energy
under Contract DE-AC05-76RL01830

Pacific Northwest National Laboratory
Richland, Washington 99352

Executive Summary

This work was performed to support performance assessment (PA) calculations for the Integrated Disposal Facility (IDF) at the Hanford Site. PA calculations require defensible estimates of physical, hydraulic, and transport parameters to simulate subsurface water flow and contaminant transport in both the near- and far-field environments. Dispersivity is one of the required transport parameters. A previous far-field data package for the IDF site recommended dispersivity values based on late-time asymptotic results from stochastic transport theory developed originally for application to saturated aquifer systems. Under steady flow conditions, transport through saturated aquifer materials is typically in the horizontal direction, parallel to stratification, whereas transport through the vadose zone (the unsaturated soil and sediment located between the ground surface and the underlying aquifer) is generally in the vertical direction, perpendicular to stratification. The latter has been observed to result in front-sharpening effects (reduced dispersion), suggesting that the dispersivity values used for vadose zone transport modeling of the IDF site be reevaluated. Use of excessively large dispersivity values for Hanford vadose zone transport modeling can result in: 1) unrealistic predictions of upward transport of contaminants (to the ground surface) against the flow in the near-field environment for the low recharge rates that are representative of the Hanford Site, 2) earlier predicted arrival times of contaminants at the water table, and 3) lower predicted peak concentrations for the far-field environment. The lower predicted peak concentrations in groundwater may not be conservative for risk assessment.

Earlier reports provided reviews of past work by others on the experimental determination of dispersivity, and new dispersivity results from experiments performed in columns packed with mixtures of non-uniform sediments from the Hanford Site. Those results, which yielded dispersivity estimates on the order of a few to tens of centimeters, are applicable to the near-field environment. The current report demonstrates methods for calculating apparent dispersivities for variably saturated porous media relevant to both near- and far-field environments using numerical flow and transport modeling, particle tracking, and moment analysis using synthetic hydraulic property fields generated with prescribed covariance models, and fields conditioned on IDF site characterization data from borehole samples. This report provides a range of calculated dispersivity values obtained for different space-time scales, levels of heterogeneity, water fluxes and tensions.

For vertical water fluxes consistent with the rates of estimated groundwater recharge rates, results obtained in the current study for short transport distances (< 1 m) are consistent with results from the earlier column experiments, with dispersivity values on the order of a few centimeters. Apparent dispersivity values obtained for larger space-time scales ($\gg 1$ m) range from a few centimeters up to almost 1 m depending on length scale, the character of heterogeneity, and the water content or saturation regime. Calculations reported herein yield dispersivity estimates similar to those used in earlier IDF PAs and provide alternative technical bases for selection of dispersivity values for future IDF PA modeling.

Acknowledgments

This work was performed for the U.S. Department of Energy Office of River Protection by Pacific Northwest National Laboratory (PNNL) under subcontract to Washington River Protection Solutions (WRPS), LLC. This work was performed for PNNL's Integrated Glass Testing Project, managed by Gary Smith (PNNL), with technical oversight by Dave Swanberg (WRPS). We thank Gary and Dave for their support. We also gratefully acknowledge Steve Yabusaki (PNNL) for providing the particle tracking code that was used in this work, Vicky Freedman, Guzel Tartakovsky, Jon Thomle, and Signe White (all PNNL) for technical reviews, and Matt Wilburn (PNNL) for editorial assistance. Finally, we thank Raz Khaleel, Gerry Grisak, and John Pickens (all Intera), Glenn Taylor and Robert Hiergesell (both SRNL), and Steve Kelly (WRPS) for providing independent external reviews of this work.

Acronyms and Abbreviations

ADE	advection-dispersion equation
IDF	Integrated Disposal Facility
PA	performance assessment
PNNL	Pacific Northwest National Laboratory
QA	quality assurance
R&D	research and development
SGSIM	Sequential Gaussian Simulation (geostatistical simulation method)
SRNL	Savannah River National Laboratory
STOMP	Subsurface Transport Over Multiple Phases (flow and transport simulator)
TVD	total variation diminishing (numerical transport scheme)
WRPS	Washington River Protection Solutions
WWFTP	WRPS Waste Form Testing Program

Contents

Executive Summary	iii
Acknowledgments.....	v
Acronyms and Abbreviations	vii
1.0 Introduction	1
1.1 Methods for Estimating Dispersivity	3
1.1.1 Stochastic-Analytical Methods.....	3
1.1.2 Particle-Based Methods.....	5
2.0 Methods	7
2.1 Physical and Hydraulic Properties	7
2.1.1 Characterization Boreholes Around the IDF.....	7
2.1.2 Sisson and Lu Site.....	9
2.1.3 Conditional Simulation of Hydraulic Parameters.....	11
2.2 Particle-Based Method for Estimation of Dispersivity	14
2.2.1 STOMP Model Setup.....	14
2.2.2 Particle Tracking	14
2.2.3 Spatial Moment Analysis	15
2.2.4 Estimation of Dispersivity.....	16
2.3 ADE-Based Method for Estimation of Dispersivity	17
2.3.1 STOMP Model Setup.....	17
2.3.2 Estimation of Dispersivity.....	20
3.0 Results and Discussion.....	20
3.1 Particle-Based Dispersivity Estimation.....	20
3.2 ADE-Based Dispersivity Estimation.....	25
4.0 Summary and Conclusions	27
5.0 Quality Assurance.....	29
6.0 References	30

Figures

Figure 1. Locations of the Hanford Site within Washington State and the 200 East Area on the Hanford Central Plateau.....	2
Figure 2. Sediment layering in a pit excavated ~175 m west of the southwest corner of the Integrated Disposal Facility. (Photograph by Dr. John Selker, Oregon State University.)	8
Figure 3. Image showing locations of the IDF Phase 1 excavation, the Sisson and Lu site, and two boreholes/wells (i.e., 299-E24-21 and 299-E17-21) from which Physical and hydraulic property data are available. (Base image from PHOENIX; http://phoenix.pnnl.gov/apps/gw/phoenix.html ; last accessed 15-Dec-2015.)	10
Figure 4. Anisotropic experimental (symbols) and model variograms for initial water content data measured on May 5, 2000, at the Sisson and Lu site (from Ward et al. 2006).....	11
Figure 5. Hydraulic parameters for (clockwise from top-left) $\ln(K_s)$ (a), α (b), n (c), θ_s (d), and θ_r (e) for SGSIM realization 5.	13
Figure 6. Miller-similar porous media with different levels of heterogeneity in $Y=\ln(K_s)$. The variance of $\ln(K_s)$ is denoted σ_Y^2 . The geometric mean of K_s for all fields is 1.0×10^{-2} cm/s (after Figure 1 of Zhang 2010).....	18
Figure 7. Variance of $\ln(K)$ as function of mean pressure head for the synthetic soils with different levels of heterogeneity. $\text{Var} = \sigma_Y^2$ and $Y = \ln(K_s)$ (after Figure 2 of Zhang 2010).	19
Figure 8. Snapshots of the locations of 5000 particles at different times for a flow field corresponding to hydraulic parameters for SGSIM realization 5 and a recharge rate of 3.5 mm/yr.....	21
Figure 9. Paths of nine selected particles from the simulation that produced Figure 10.	22
Figure 10. Apparent dispersivity in the vertical direction for three realizations of hydraulic parameters and three recharge rates.	23
Figure 11. Solute longitudinal dispersivity (a) under 1-D heterogeneity and (b) 3-D heterogeneity conditions. The 1-D results were based on 10 simulations and the 3-D results were based on 3 simulations. For the 1-D, $h = -1.5$ m scenarios (plot a3, the breakthrough for V3.0 and V4.0 did not occur because the flow rates were too low. The vertical bars indicate one standard deviation.	25
Figure 12. Impacts of soil spatial variability on solute longitudinal dispersivity at 4 m for 1-D and 3-D heterogeneity conditions. The 1-D results were based on 10 simulations and the 3-D results were based on 3 simulations. For the 1-D, $h = -1.5$ m scenarios (plot c), solute breakthrough for V3.0 and V4.0 did not occur because the flow rates were too low.	26

Tables

Table 1. Nested spherical variogram model for initial water content data measured on May 5, 2000, at the Sisson and Lu site (from Ward et al. 2006).....	11
Table 2. Calculated apparent values of dispersivity in three directions for realization 5.	24
Table 3. Estimated longitudinal (A_{zz}) and transverse (A_{xx} , A_{yy}) dispersivity values for the IDF site.....	24

1.0 Introduction

The U.S. Department of Energy is responsible for the safe treatment and long-term disposal of radioactive and other hazardous wastes that resulted from former nuclear weapons production activities at the Hanford Site in southeastern Washington State (Figure 1). The Integrated Disposal Facility (IDF), located at the southern end of the 200 East Area of the Hanford Site, will be used for disposal of wastes from underground storage tanks. Current plans call for the bulk of the tank waste to be pretreated, immobilized, and stored as a low-activity vitrified (glass) waste form. Secondary waste and ancillary equipment may also be disposed of in a cast stone (a grout-like material) or other supplemental waste form. The vitrified and supplemental waste will be co-disposed of at the IDF.

Assessing the long-term performance of the IDF and the potential risk associated with the waste inventory planned for this facility requires the use of computer models to simulate water flow and contaminant transport through the subsurface. These models require parameters to describe the physical, hydraulic, geochemical, and transport properties of both the natural and the engineered components of the system. Risk assessments for Hanford waste sites generally show that contaminants accessed through the groundwater pathway are the most significant potential risk drivers. Therefore, it is important to accurately estimate the parameters used in the subsurface flow and transport models to provide defensible assessments of IDF performance and risk. Dispersivity is one of the parameters required for subsurface transport modeling.

The objective of this work was to estimate dispersivities for variably saturated sediments representative of those underlying the IDF site, applicable to future contaminant transport modeling used for site performance and risk assessment. This report is organized as follows. The remainder of Section 1.0 focuses on a review of literature relevant to estimating dispersivities for variably saturated porous media. Section 2.0 describes the specific methods that were used in this study. Results and discussion are provided in Section 3.0, and the work is summarized in Section 4.0.

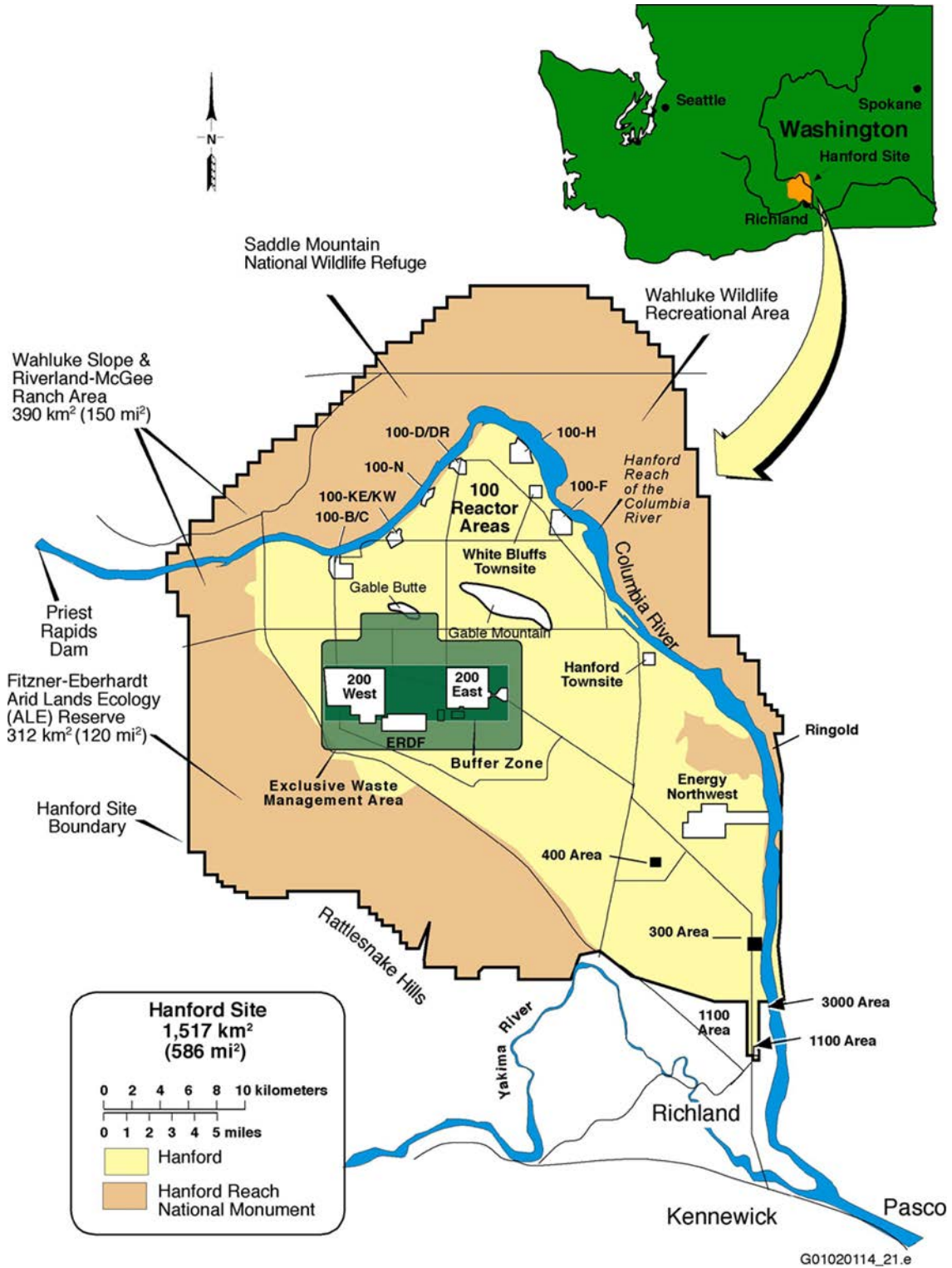


Figure 1. Locations of the Hanford Site within Washington State and the 200 East Area on the Hanford Central Plateau.

1.1 Methods for Estimating Dispersivity

The advection-dispersion equation (ADE) has become an accepted model for solute transport in both saturated and unsaturated porous media. However, no practical methods or guidelines have been developed for estimating scale-dependent dispersivity values in the ADE for vadose zone transport modeling. This is partly because most vadose zone modeling applications represent relatively shallow sites associated with agriculture, for which the ADE can be directly fit to field transport data to estimate dispersivity (Jury and Roth 1990). Very little experimental or numerical work has been done to quantify scale-dependent solute dispersion effects for highly heterogeneous variably saturated porous media over the range of space-time scales relevant to waste management concerns at Hanford.

Difficulties in estimating both flow and transport parameters for Hanford Site performance assessment applications stem from the very large spatial and temporal scales of interest for modeling, the highly heterogeneous nature of the subsurface, and the sparsity of vadose zone characterization and monitoring data. The predominantly coarse and unconsolidated nature of sediments in the vadose zone, which approaches 100 m thick in some areas of the Hanford Central Plateau (the “Exclusive Waste Management Area” shown in Figure 1), also makes it difficult to collect minimally disturbed and representative samples. Consequently, dispersivity values needed for large-scale vadose zone transport modeling at Hanford have been estimated in the past using theoretical results from stochastic-analytical methods developed originally for application to saturated aquifer systems (Gelhar and Axness 1983; Khaleel et al. 2000; Khaleel 2004).

Transport in aquifers occurs predominantly in a direction parallel to the stratification of the porous media. The solute dispersion process is more complicated in the vadose zone because the principal transport direction is usually perpendicular to stratification and dispersion is also influenced by variable water content, which is a non-linear function of the matric potential and associated flux conditions. Experimental results for transport perpendicular to stratification in strongly layered vadose zone sediments have been shown to exhibit front-sharpening effects (reduced dispersion) that are counter to observations typically seen for transport parallel to stratification in saturated aquifer systems (Porro et al. 1993). Laboratory experimental studies for variably saturated porous media also indicate that dispersivity increases with decreasing water content or saturation (Padilla et al. 1999; Nützmann et al. 2002).

The reported differences between dispersion effects observed in saturated aquifer systems and in unsaturated porous media motivated the current study to evaluate alternative methods for estimating dispersivity in support of performance assessment modeling activities for the IDF site. The remainder of this section provides a brief review of some numerical methods that have been applied to estimate dispersivity for variably saturated porous media.

1.1.1 Stochastic-Analytical Methods

Scale-dependent solute dispersion in saturated aquifer systems is a well-known phenomenon that has been studied extensively using results developed from stochastic-analytical methods (Gelhar and Axness 1983; Dagan 1984; Gelhar 1993). Gelhar et al. (1994, p.15) note, however, that “there is no scientific consensus about how to characterize dispersion in unsaturated flow.” Comparisons of deterministic and stochastic model predictions with validation data from a field experiment performed in unsaturated soils at the Las Cruces Trench Site in New Mexico led to the following additional comments:

“Certainly, the results of the test raise questions about the validity of basing long-term performance assessments on the deterministic predictions, which seem to degrade over time. On the other hand, the results are too inconclusive to lend much credibility to the stochastic model” (Gelhar et al. 1994, p. 53).

Since the early work of Gelhar and co-workers with saturated porous media systems, several additional numerical studies have evaluated water flow and solute transport and dispersion in variably saturated porous media based on stochastic-analytical methods (Mantoglou and Gelhar 1985; Polmann 1990; Gelhar et al. 1994). Subsequent work included Yang et al. (1996), who evaluated the effects of spatially variable water content on solute transport in gravity-dominated flow (unit hydraulic gradient) through heterogeneous porous media, and derived analytical expressions for macrodispersivity. However, they neglected the functional dependence of unsaturated hydraulic conductivity and water content on pressure head, replacing the normally spatially variable pressure head with a mean value. Harter and Zhang (1999) performed a similar analysis that considered both the spatial variability of pressure head and the associated water content. Additional related work for variably saturated porous media is described by Russo (1993, 1998, 2003).

For analytical tractability, many of the studies noted above used the Gardner (1958) model of unsaturated hydraulic conductivity and the Russo (1988) model of water retention, both of which are exponential functions of pressure head. These studies have shown that the spatial variability of water content may have significant impacts on the velocity covariance and resulting estimates of macrodispersivity. The Brooks and Corey (1964) and van Genuchten (1980) functions are generally preferred in practice because they typically provide more accurate representations of measured water retention and unsaturated hydraulic conductivity data. However, the non-linearity of the van Genuchten (1980) function, and the non-linearity of associated hydraulic conductivity functions (Mualem 1976), has generally precluded their use in stochastic-analytical methods for flow and transport in variably saturated porous media.

Concerns about whether results obtained using existing stochastic-analytical methods are applicable to the Hanford vadose zone stem from 1) differences between soil/sediment types represented in earlier studies and those at Hanford, since Hanford sediments are generally much coarser and more heterogeneous than shallow agricultural soils, 2) the common use in many earlier studies of simplified constitutive relations for the soil hydraulic properties, and 3) the assumption of small variability implied by the use of perturbation analysis in the development of results for stochastic-analytical methods.

Regarding the use of simplified constitutive relations for soil hydraulic properties in the development of stochastic-analytical solutions, Zhang et al. (1998) developed first-order stochastic models for vertical (1-D), gravity-dominated (unsaturated) flow in second-order stationary porous media using both the Gardner-Russo and Brooks and Corey (1964) models. They showed that the mean head and mean effective water content for the Brooks-Corey model (a power function) differ substantially from the Gardner-Russo models (exponential functions) near both the dry and wet limits, while differences were smaller at intermediate saturations. The Brooks-Corey model was found to provide certain advantages in the development of analytical solutions. The stochastic model developed for the Brooks-Corey functions requires the coefficient of variation of head and water entry pressure to be small ($\ll 1$), whereas the model based on the Gardner-Russo functions assumes the one-point cross-covariance of the head and Gardner-Russo alpha parameter to be small ($\ll 1$). Zhang et al. (1998) showed that the latter condition

may be violated because the one-point covariance increases rapidly to beyond unity as the soil becomes dry, whereas the requirements for the Brooks-Corey functions may be more readily satisfied.

Khaleel et al. (2002) performed Monte Carlo simulations of steady flow and transient solute transport in two-dimensional variably saturated porous media to test the applicability of stochastic-analytical solutions for estimating macrodispersivity in vadose zone sediments. A 20-m-wide by 20-m-deep model domain was used with spatially-variable hydraulic properties that were similar to those of the sandy sediments at the IDF site (Khaleel 2004). Dispersivities were computed for steady flow both parallel and perpendicular to sediment stratification using the spatial moments of concentration distributions determined using the modified method of characteristics (MMOC) numerical technique. Results for flow parallel to stratification were obtained by rotating the model domain and associated material properties by 90 degrees.

Khaleel et al. (2002) computed values of macrodispersivity from the spatial moments of their ensemble-mean concentration plumes. They obtained dispersivity values perpendicular to bedding that were on the order of tens of cm at tensions of up to 2 m. For these relatively low tensions, macrodispersivity values estimated from the analytical expressions of Mantoglous and Gelhar (1985) were greater than, but of the same order of magnitude as, the ensemble mean plume results. However, the stochastic based solutions were shown to diverge quickly from the ensemble averages at higher tensions. For flow and transport parallel to bedding and tensions up to 2 m, they obtained dispersivity values on the order of 1 m. At higher tensions Khaleel et al. (2002) noted considerable disagreement between the ensemble averages and the stochastic results, with the stochastic macrodispersivities being much larger than the ensemble average results. Khaleel et al. (2002, p. 11-11) concluded that, "The lack of a reasonable agreement between the numerical and stochastic solutions at high tensions raises questions about vadose zone dispersivities being defined in a manner similar to those for saturated media." However, Khaleel (2004) then used the analytical formula developed by Gelhar and Axness (1983), to estimate longitudinal macrodispersivity values of 2 m and 0.3 m for the unsaturated sandy and gravelly sediments, respectively, at the IDF site.

Khaleel et al. (2002) reported values of macrodispersivity for different mean tensions, but did not show how their macrodispersion coefficients changed with increasing transport distance. Therefore the extent to which the results by Khaleel et al. (2002) might represent asymptotic conditions is unknown. Dagan (1989, p. 318) states that "the asymptotic regime is reached for a travel distance of the order of 50 integral scales...". Khaleel (2004) estimated a vertical correlation length for $\ln(K_s)$ of the sandy sediments at the IDF site of 0.3 m. If the correlation length for an exponential variogram model with zero nugget is equated with integral scale (Western and Blöschl, 1999), a first estimate of the vertical transport distance at which asymptotic macrodispersivities might be obtained for the IDF site is $50 \times 0.3 \text{ m} = 15 \text{ m}$.

1.1.2 Particle-Based Methods

Cirpka and Kitanidis (2002) described an alternative to stochastic-analytical methods for estimating dispersivity in variably saturated porous media. Their methodology is based on one- and two-particle travel time statistics for estimating dispersivities for unsaturated porous media under steady vertical flow conditions. An advantage of particle-based methods over stochastic-analytical methods is that they do not depend on the use of any particular functional form for the hydraulic properties, or their spatial correlation structure, and there are no restrictions on the ranges of variability. The methodology described

by Cirpka and Kitanidis (2002) considered the cross-correlation between van Genuchten (1980) model hydraulic parameters (but with constant porosity) using parameter distributions and transformations from Carsel and Parrish (1988).

Parametric models were developed by Cirpka and Kitanidis (2002) by fitting their particle tracking results to estimate “macro” dispersivities, based on simulated one-particle travel-time variances, and “effective” dispersivities based on two-particle displacement covariances. The different methods and names were used to distinguish between particle dispersion resulting from advection only and advection with molecular diffusion and dilution. The effects of these different processes can potentially be distinguished using these one- and two-particle methods which are also discussed by Dagan (1989). Note, however, that the terms “macro” and “effective” are not used consistently in the literature, and macrodispersivity does not necessarily imply that asymptotic conditions have been reached. The additional terms “longitudinal” and “transverse” that are used with dispersivity refer to dispersivity for the mean flow direction and in the orthogonal directions, respectively. The results described by Cirpka and Kitanidis (2002) represent longitudinal dispersivities in the vertical flow direction.

Cirpka and Kitanidis (2002) showed dispersivities to be functions of both the transport distance and the vertical specific discharge (net infiltration) rate. For their hypothetical silt loam soil with a mean tension of 0.3 m, fitted macro-dispersivities for the parametric model reached constant (asymptotic) values of ~0.17 m after a vertical transport distance of ~2 m. The maximum macro- and effective dispersivity values obtained from the particle travel time statistics at a 4-m vertical travel distance were ~0.25 m and ~0.15 m, respectively. Note that the vertical extent of the domain of interest for IDF PA calculations is 15-20 times longer than the vertical extent of the model domain evaluated by Cirpka and Kitanidis (2002). However, if asymptotic (constant) dispersivity values are achieved at shorter transport distances, the results would be applicable to larger scales.

The parametric equations for dispersivity developed by Cirpka and Kitanidis (2002) required the vertical specific discharge (net infiltration or recharge rate) plus 10 additional parameters that were estimated by fitting particle travel time results. This is in addition to the parameters required for describing the distribution of soil hydraulic properties that were used to generate the flow fields. Overall, the methodology developed by Cirpka and Kitanidis (2002) appears robust, and broadly applicable, but it is computationally intensive and was demonstrated for only a single hypothetical soil type (silt loam). Meyer et al. (1997) provide alternative parameter distributions and cross-correlation coefficients for van Genuchten (1980) model parameters for different soil types based on the database of Carsel and Parrish (1988). The information in Meyer et al. (1997) could potentially be used to perform additional analyses similar to those of Cirpka and Kitanidis (2002), but for other soil types. Performing such analyses and compiling the results for a wide range of soil types could potentially provide a valuable resource for future vadose zone transport modeling at Hanford and elsewhere.

Several other particle-based approaches for estimating dispersivities in variably saturated porous media are described by Jury and Roth (1990). These include methods based on both temporal moment analysis and spatial moment analysis. One advantage of using temporal moments, such as the methods described by Cirpka and Kitanidis (2002), is that travel times can be computed for the entire length of the domain of interest along the principal transport direction. Spatial moment analysis is strictly applicable to space-time scales for which all of the particles remain within the model domain. This effectively means that spatial moment analysis requires a larger model domain, and/or for a given domain size the results from spatial moment analysis are valid for shorter space-time scales relative to temporal moment analysis.

However, spatial moment analysis has the advantage over temporal moment analysis of allowing dispersivity values to be estimated for all principal directions simultaneously, whereas temporal moment analysis is applicable only to the direction of mean transport. Freyberg (1986) describes a case study on application of spatial moment analysis to estimate dispersivity of saturated sediments for the Borden Aquifer in Ontario, Canada. Methods used to estimate both hydraulic parameters and dispersivities for the current study are described in the following section.

2.0 Methods

Flow and transport properties and parameters for variably saturated systems are inextricably linked, since the variability of hydraulic conductivity and water content affect the pore water velocities and associated solute dispersion. However, if spatially distributed estimates of hydraulic parameters are available or can be generated from site characterization data, particle-tracking and moment-based methods can be applied to estimate dispersivity. This section describes methods that were used to generate estimates of spatially variable hydraulic parameters, followed by descriptions of the methods used to estimate dispersivity.

2.1 Physical and Hydraulic Properties

The cataclysmic flood events that deposited the sediments at the Hanford Site produced a highly variable distribution of sediment structures and textures (Bjornstad 2006). Figure 2, after Fayer and Szecsody (2004), shows a photograph of the face of a trench excavated ~174 m west of the southwest corner of the IDF. This figure illustrates the potentially heterogeneous nature of the subsurface that could underlie the IDF.

The general character of subsurface sediments observed in boreholes drilled around the IDF was described by Reidel (2005). Characteristics of sediments exposed on the walls and base of the pit for the IDF Phase 1 excavation are described by Reidel and Fecht (2005). The interbedded sands and silts mapped by Reidel and Fecht (2005) appear to be similar to those seen at the excavation depicted in Figure 2. Reidel and Fecht (2005) also mapped the locations of several clastic dikes that cut through the IDF. No characterization data are available for the region immediately underlying the footprint of the IDF, so data from nearby sites were used to estimate properties for the IDF site.

2.1.1 Characterization Boreholes Around the IDF

Physical and hydraulic property characterization data were measured for core samples obtained from several boreholes/wells around the area of the IDF (Reidel 2005; Khaleel 2004). Figure 3 shows the locations of the two primary characterization wells, 299-E17-21 and 299-E24-21, which are located to the southwest and northeast of the current IDF Phase 1 excavation, respectively. Hydraulic parameters determined for 41 core samples from these wells were used in the current study (see Rockhold et al. 2015b, Table 6.3). The spacing of core samples for the boreholes around the IDF is inadequate for reliable determination of spatial auto- and cross-correlation. Therefore, information on spatial correlation structure from another site was used.

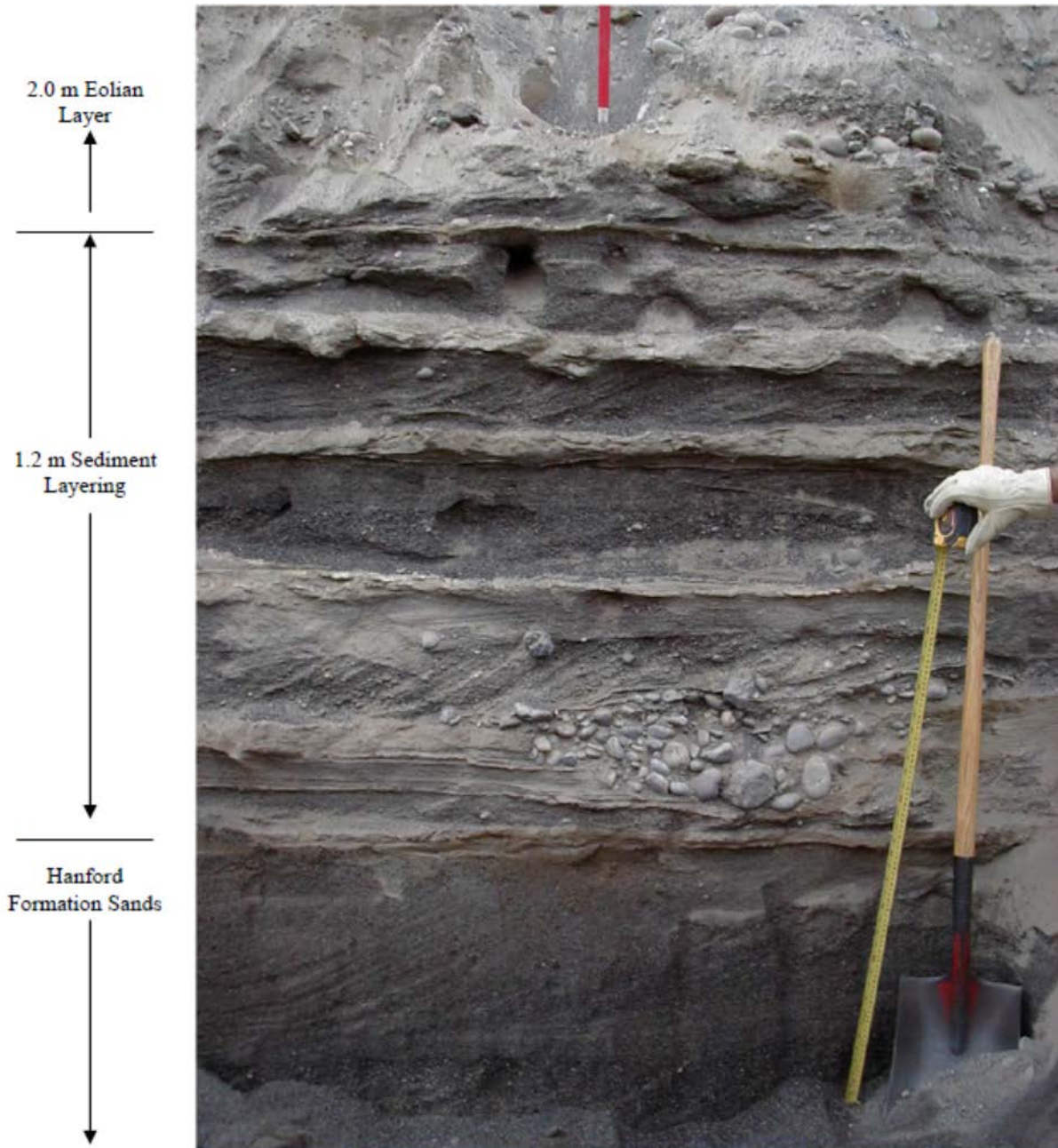


Figure 2. Sediment layering in a pit excavated ~175 m west of the southwest corner of the Integrated Disposal Facility. (Photograph by Dr. John Selker, Oregon State University.)

There are only two sites at Hanford where detailed characterization and field experiments have been performed to evaluate the influence of heterogeneous sediments on water flow and solute transport behavior at relatively large scales in the vadose zone. These are the Sisson and Lu site (Sisson and Lu 1984; Fayer et al. 1995) and the Army Loop Road site (Ward et al. 2006; Ward and Zhang 2007). Although information on cross-correlation of hydraulic parameters, and autocorrelation of hydraulic parameters in the horizontal direction, is available for Army Loop Road site, no information on vertical correlation lengths is available from that site. The Army Loop Road site is also farther away (~6.5 km)

from the IDF than is the Sisson and Lu site (~200 m). Therefore, information on spatial correlation of sediment properties from the Sisson and Lu site was used in the current study.

2.1.2 Sisson and Lu Site

The Sisson and Lu site is located approximately 200 m to the east of the IDF (Figure 3). The original field site was instrumented with thirty-two 18-m-deep steel monitoring wells that were used to measure soil moisture and activity of radioactive solutes for subsurface injection experiments. Characterization and monitoring were performed from the steel cased wells using neutron-moisture and other wire-line geophysical logging tools (Sisson and Lu 1984; Fayer et al. 1995). A shallow (~3.6-m-deep) injection well in the middle of the site that was used for point-source injections of both conservative tracers and sorbing solutes (e.g., Cs, Sr). Additional field experiments were performed at the Sisson and Lu site in 2000 and 2001 to evaluate flow and transport behavior for different fluids and to test different geophysical monitoring technologies (Ward et al. 2006). Sampling and physical and hydraulic property characterization data from the Sisson and Lu site are described by Last and Caldwell (2001) and Schaap et al. (2003), respectively.

The solute transport results from experiments performed at the Sisson and Lu site are insufficient for evaluating field-scale dispersion, due to limited monitoring in both space and time. However, the water content data from the Sisson and Lu site have been used successfully for evaluating spatial auto-correlation structure of water content (Ward et al. 2006) and for indirect determination of hydraulic parameters for field-scale modeling (Rockhold 1999). Experimental results from the Sisson and Lu site have also been used for developing alternative models for saturation-dependent anisotropy of hydraulic conductivity (Zhang et al. 2003; Zhang and Khaleel 2010; Rockhold et al. 2015b).

2.1.2.1 Spatial Auto- and Cross-Correlation

In general, physical and hydraulic property data for samples collected from Hanford boreholes/wells are very limited. When core or grab samples are obtained from a borehole, the vertical sample frequency is often limited to a minimum of ~1.5 m (~5 ft) depth intervals, and sampling is often not performed over the entire length of the borehole. The limited sampling frequency is insufficient for resolving smaller-scale features such as those shown in Figure 2, which control subsurface flow and transport behavior. Distances between boreholes/wells are also typically quite large, perhaps hundreds of meters, as shown in Figure 3. Therefore, the data needed for quantitatively evaluating spatial auto- and cross-correlation is usually lacking. However, results from the Sisson and Lu site, which has much higher sample density, may be representative and transferrable to the IDF site. Density log measurements were made in thirty-two, 18-m-deep wells at the Sisson and Lu Site, at 0.025 and 0.15 m vertical spacings. Neutron moisture and gamma log measurements were also made in these wells at 0.15 m spacings. Hydraulic property measurements were also made on approximately 60 core samples from this site. Owing to the limited data available for the IDF site, variogram models determined using the initial water content distribution from the Sisson and Lu site on May 5, 2000 (Ward et al. 2006; Table 2.10) were used as surrogates to define the spatial autocorrelation structure of hydraulic properties for the subsurface underlying the IDF site. This represents the water content distribution under dry, ambient conditions, prior to water injections for the experiment performed in 2000.



Figure 3. Image showing locations of the IDF Phase 1 excavation, the Sisson and Lu site, and two boreholes/wells (i.e., 299-E24-21 and 299-E17-21) from which Physical and hydraulic property data are available. (Base image from PHOENIX; <http://phoenix.pnnl.gov/apps/gw/phoenix.html>; last accessed 15-Dec-2015.)

A precedence for using the spatial variability of field-measured water content data as a surrogate for the spatial variability of hydraulic parameters was established by Rockhold et al. (1996), using characterization data and modeling of field experiments at the arid Las Cruces Trench Site in New Mexico. The spatial correlation structures of the initial water content data and of scale factors representing the saturated hydraulic conductivity and air-entry pressure of core samples from that site were very similar, to the extent that the initial water content data could be used to estimate hydraulic parameters (Rockhold et al. 1996). A similar approach was applied successfully for parameterization of a vadose zone flow model for simulation of the original field injection experiment performed at the Sisson and Lu site (Rockhold 1999).

Figure 4 shows the variogram models for the May 5, 2000, water content data set from the Sisson and Lu site, representing the spatial variability of water content under dry, ambient conditions prior to water

injections for the field experiment (Ward et al. 2006). Table 1 lists the nested spherical variogram model parameters. The spatial auto-correlation structure of water content at this site is anisotropic in the horizontal plane as well as between the horizontal plane and vertical direction. The azimuth defining the direction of maximum spatial continuity in the horizontal plane is 22.5 degrees. This orientation is orthogonal to the assumed primary direction of water flow (from NW to SE) during the cataclysmic flooding events that deposited the Hanford formation sediments, which is consistent with depositional environment. The variogram models depicted in Figure 4 were applied to estimate spatially distributed hydraulic parameter fields for use in estimating dispersivity to represent the IDF site.

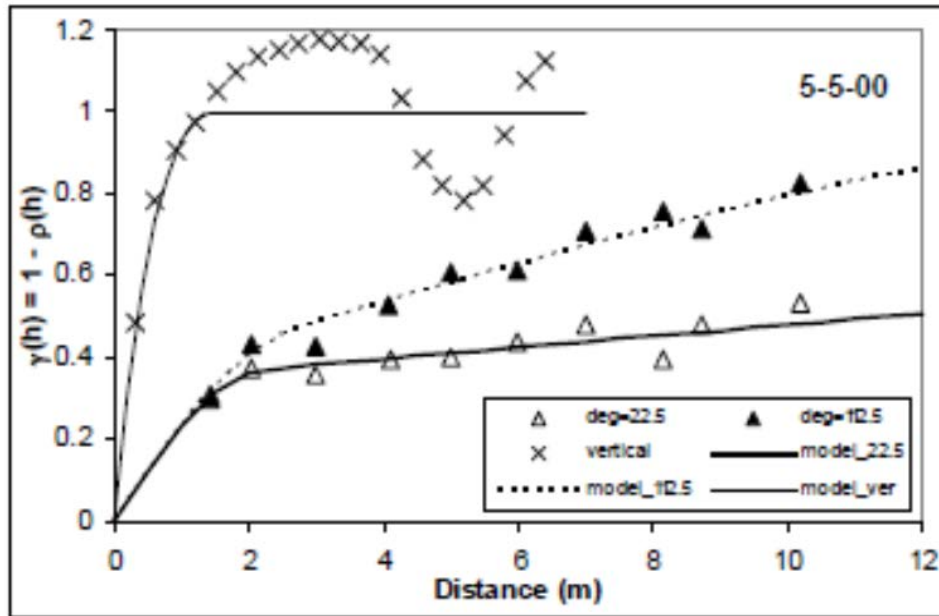


Figure 4. Anisotropic experimental (symbols) and model variograms for initial water content data measured on May 5, 2000, at the Sisson and Lu site (from Ward et al. 2006). The parameter ρ is the autocorrelation coefficient at lag (distance) h , and γ is the semi-variance computed as one minus the autocorrelation.

Table 1. Nested spherical variogram model for initial water content data measured on May 5, 2000, at the Sisson and Lu site (from Ward et al. 2006).

Nugget	Variogram Model	Sill	Range (m)		
			Deg. = 22.5	Deg. = 112.5	Vertical
0	Spherical	0.34	2.2	2.7	0.6
	Spherical	0.66	70	20	1.4

2.1.3 Conditional Simulation of Hydraulic Parameters

Hydraulic parameters determined on core samples collected during the drilling of well 299-E17-21 were used in conjunction with the variogram model shown in Figure 4, whose parameters are listed in Table 1, to generate conditional simulations of hydraulic parameters. The sequential Gaussian simulation method implemented in the Sequential Gaussian Simulation (SGSIM) program was used (Deutsch and

Journal 1998). Conditionally simulated fields were simulated for the five hydraulic parameters, $\ln(K_s)$, α , n , θ_s , θ_r , corresponding to the van Genuchten (1980) water retention and Mualem (1976) hydraulic conductivity functions.

Conditional simulation results were generated for a 25-m (X) by 25-m (Y) by 50-m (Z) domain with uniform 0.25-m spacing between grid points in each coordinate direction (2,000,000 grid points). The domain size was selected to provide representative results for the sandy sediments underlying the IDF. The implied support volume for each point in the geostatistical simulations is approximately equal to the volume of interrogation of neutron probe measurements of soil moisture in the field (Fayer et al. 1995), but slightly larger than the typical size of a core sample (~0.1-m diameter by ~0.2-m long). Borehole neutron moisture and spectral gamma log data represent the data types with the highest (vertical) spatial sampling frequency available for the Hanford Site. Therefore, these data typically provide more information about the spatial structure and variability of sediment properties than any other available data. It is well known, however, that spatial variability is manifested over a hierarchy of scales from molecular to pore, grain, core and up to field scales. The same variogram model parameters from Table 1 were applied to generate each of the five hydraulic parameters, but the fields for each parameter were conditioned on the values of that parameter determined from core samples collected from well 299-E17-21, located at the southwest corner of the domain used for the conditional simulations.

Results for one realization are shown in Figure 5. Note that the layered structure of the hydraulic parameters shown in Figure 5 appears to be similar to layering illustrated in the photograph in Figure 2 for the excavation near the IDF. The conditionally simulated hydraulic parameter fields were used with the STOMP (Subsurface Transport Over Multiple Phases) simulator (White and Oostrom 2000; White et al. 2015) to generate steady state flow fields. The flow fields were then used for particle tracking and dispersivity calculations as described in the following subsection.

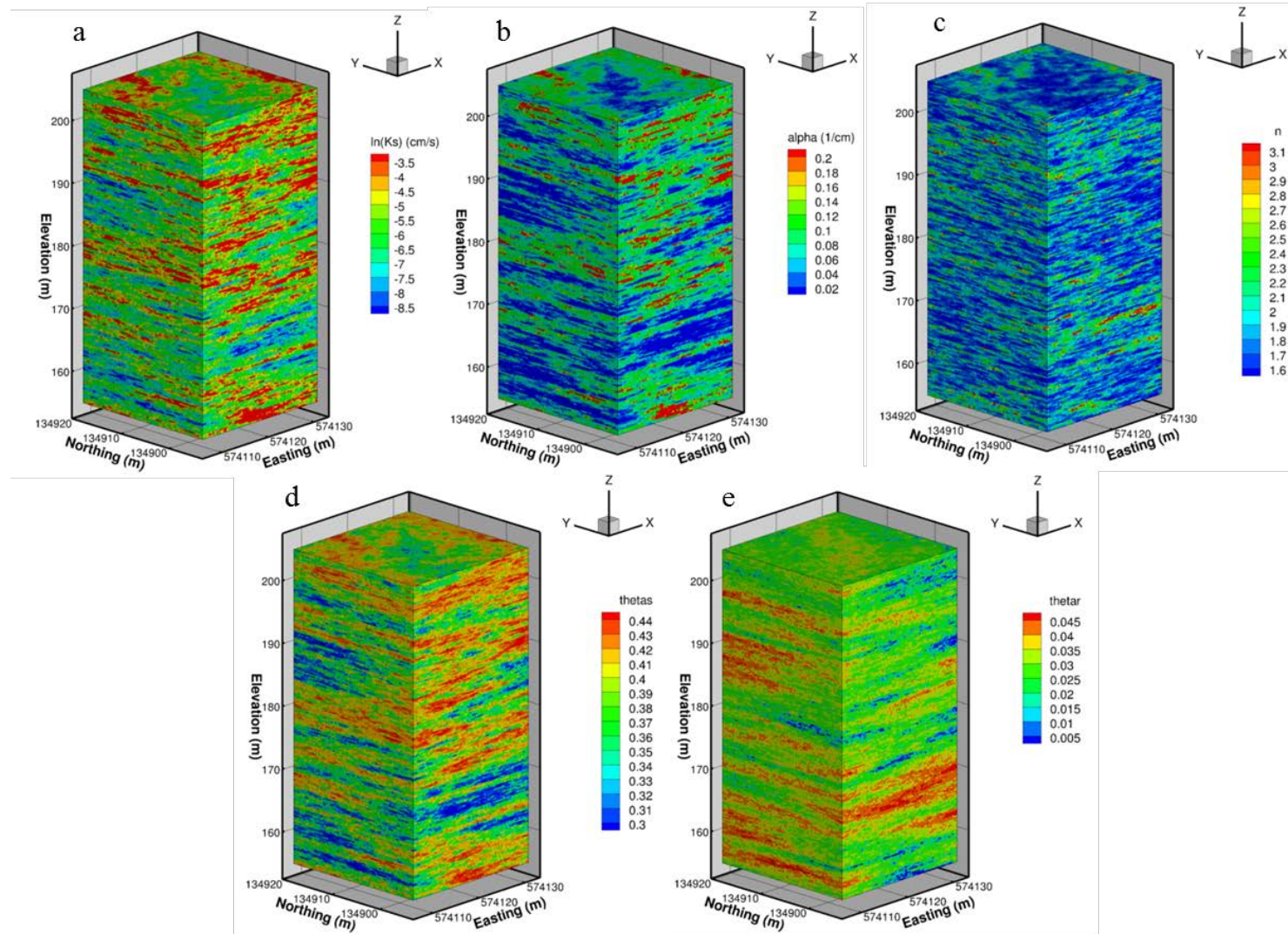


Figure 5. Hydraulic parameters for (clockwise from top-left) the natural log of the saturated hydraulic conductivity, $\ln(K_s)$ (a), the van Genuchten (1980) model α parameter (b), the van Genuchten (1980) model n parameter (c), the saturated water content, θ_s (d), and the residual water content, θ_r (e) for SGSIM realization 5.

2.2 Particle-Based Method for Estimation of Dispersivity

The *particle-based method* used for estimation of dispersivity consisted of the following steps:

1. Run steady-state flow simulations with STOMP using the generated hydraulic parameter fields (Section 2.1.3) to obtain velocity and water content distributions for a range of prescribed upper boundary conditions (different recharge rates).
2. Perform particle tracking (advection only) through the simulated steady-state flow fields.
3. Calculate spatial moments of the particle distributions, and estimate dispersivities from the time rate of change of the second spatial moments.

Each step is described in more detail below.

2.2.1 STOMP Model Setup

Numerical simulations related to the particle-based estimation of dispersivity were performed with a 25-m by 25-m by 25-m model domain, discretized with uniform 0.25 m grid spacing in each direction, yielding 10^6 model grid blocks. The STOMP simulator was used because it provided Darcy velocities on cell faces, which are not currently available for output from the scalable version of the code (eSTOMP). To reduce simulation times, only the lower half of the domain shown in Figure 5 was simulated. Note that the three-dimensional model domain used here for the particle-based method is 20% larger in the X- and Z-directions than that used for two-dimensional simulations reported previously by Khaleel et al. (2002). Calculations noted earlier suggest that asymptotic conditions for the IDF site could possibly be obtained within a vertical transport distance of ~15 m. Results reported by Khaleel et al. (2002) for flow perpendicular and parallel to bedding, and observations of front-sharpening effects reported in the literature for vertical transport through horizontally-stratified vadose zone sediments (Porro et al. 1993), suggest that asymptotic conditions might be obtained for shorter transport distances.

Neumann-type (prescribed flux) boundary conditions were specified for the upper boundary of the domains used for STOMP simulations. Three different fluxes were used, corresponding to recharge rates of 0.5, 1, and 3.5 mm/yr. These recharge rates are thought to be representative of undisturbed areas with native shrub-steppe vegetation near the IDF (Fayer and Szecsody 2004). Simulations were performed using three stochastic realizations of the hydraulic parameter fields to illustrate some of the potential variability and uncertainty in results. Neumann-type, zero-flux boundary conditions were specified for all side boundaries. A unit hydraulic gradient was specified for the lower boundary, which is located above the water table for the domain represented in these simulations.

2.2.2 Particle Tracking

Particle tracking was performed with the flow fields generated by STOMP using a purely advective, semi-analytical method (Pollock 1988; Scheibe and Yabusaki 1998). The method assumes that each directional velocity component varies linearly within a grid cell for each coordinate direction. This allows for an analytical expression describing the flow path within individual grid cells. Given the initial position of a particle within a grid cell, the coordinates of the particle at any other point within the cell and the time of travel to get there can be directly computed. The method allows for the path of particles to be

traced through any multidimensional flow field generated from block-centered finite difference type flow models. The implementation used here assumes uniform grid spacing in each coordinate direction and was applied to flow fields generated by STOMP. Use of a purely advective particle tracking method has the advantage over numerically solving the ADE because numerical dispersion is not introduced into the results.

Five thousand particles were initially placed 0.05 m from the upper boundary of the model domain at time zero, but with no particles initially located within a distance of less than 25% of the minimum and maximum X and Y dimensions (i.e., all particles were initially placed near the top boundary but >6.25 m away from the sides of the model domain). This initial particle placement was selected to reduce the effects of boundary conditions on the results. Particles were tracked until they exited the lower boundary of the model domain.

2.2.3 Spatial Moment Analysis

The evolution of particle clouds generated using the particle tracking algorithm was evaluated using spatial moment analysis (Aris 1956). The following description is adapted from Freyberg (1986) for calculation of the spatial moments of particle distributions.

The ijk^{th} moment of a distribution of particles in space is defined as

$$M_{ijk}(t) = \int_{-\infty}^{\infty} \int_{-\infty}^{\infty} \int_{-\infty}^{\infty} x(t)^i y(t)^j z(t)^k dx dy dz \quad (1)$$

where x , y , and z are the spatial coordinates of a particle, and t is time. The zeroth, first, and second ($i + j + k = 0, 1$, or 2 , respectively) spatial moments of particle distributions were computed to measure the total number of particles, the center of mass, and spread of the particle distribution about its center of mass. The zeroth moment, M_{000} , is equal to the total mass or total number of particles in the domain. The first moment, normalized by the zeroth moment, defines the location of the center of mass (x_c, y_c, z_c):

$$x_c = \frac{M_{100}}{M_{000}} \quad y_c = \frac{M_{010}}{M_{000}} \quad z_c = \frac{M_{001}}{M_{000}} \quad (2)$$

The second moment about the center of mass defines a spatial covariance tensor:

$$\sigma^2 = \begin{bmatrix} \sigma_{xx}^2 & \sigma_{xy}^2 & \sigma_{xz}^2 \\ \sigma_{yx}^2 & \sigma_{yy}^2 & \sigma_{yz}^2 \\ \sigma_{zx}^2 & \sigma_{zy}^2 & \sigma_{zz}^2 \end{bmatrix}$$

$$\sigma_{xx}^2 = \frac{M_{200}}{M_{000}} - x_c^2 \quad \sigma_{yy}^2 = \frac{M_{020}}{M_{000}} - y_c^2 \quad \sigma_{zz}^2 = \frac{M_{002}}{M_{000}} - z_c^2$$

$$\sigma_{xy}^2 = \sigma_{yx}^2 = \frac{M_{110}}{M_{000}} - x_c y_c \quad \sigma_{xz}^2 = \sigma_{zx}^2 = \frac{M_{101}}{M_{000}} - x_c z_c \quad \sigma_{yz}^2 = \sigma_{zy}^2 = \frac{M_{011}}{M_{000}} - y_c z_c \quad (3)$$

The components of the spatial covariance tensor are related to the spread of the particle distribution about its center of mass.

2.2.4 Estimation of Dispersivity

Under steady flow conditions with uniform velocity and transport governed by the ADE, the dispersion coefficient tensor (\mathbf{D}) and time rate of change of the covariance tensor are related by (Aris 1956; Freyberg 1986)

$$\mathbf{D} = \frac{1}{2} \frac{d}{dt} (\sigma^2) \quad (4)$$

The dispersion coefficient tensor is related to pore-water velocity by (Bear 1972)

$$\mathbf{D} = D_d \mathbf{I} + \mathbf{A} |V| \quad (5)$$

where D_d is the coefficient of molecular diffusion of the solute in the porous media, \mathbf{I} is an identity matrix, $|V|$ is the magnitude of the velocity vector, and \mathbf{A} is the dispersivity tensor. If D_d is assumed to be negligible relative to the second term on the right side of Eq. (5), the dispersivity can be estimated from the covariance tensor as (Güven et al. 1984)

$$\mathbf{A} = \frac{1}{2|V|} \frac{d}{dt} (\sigma^2) \quad (6)$$

If the movement of particles through a flow field is consistent on average with that predicted by the conventional ADE with mean velocity and constant \mathbf{D} , then the apparent dispersivity can be estimated from Eq. (6) using the slope of a line fit to the σ^2 versus time data. Dispersivity values estimated in this way would represent average values over the period and associated travel distance that is evaluated (Freyberg 1986).

Alternatively, the apparent dispersivity in the vertical direction may be estimated over discrete time intervals using

$$A_{zz}(t) = \frac{1}{2|U|} \frac{\sigma_{zz}^2(t) - \sigma_{zz}^2(t_e)}{t - t_e} \quad (7)$$

where t and t_e are some time and an earlier time, respectively, at which the spatial moments of the particle clouds are evaluated, and $|U|$ is the magnitude of the velocity vector computed from the time rate of change of the center of mass of the particle distribution. Equation (7) was used to evaluate the evolution of apparent dispersivity for the vertical direction over space-time for simulated flow fields generated with STOMP. The starting time for evaluation of Eq. (7) was year 1. Apparent dispersivities in the orthogonal directions can also be estimated by substituting σ_{xx}^2 or σ_{yy}^2 for σ_{zz}^2 in Eq. (7).

2.3 ADE-Based Method for Estimation of Dispersivity

The ADE-based method for estimating dispersivity consisted of the following steps:

1. Run steady-state flow simulations with STOMP using spatially variable hydraulic parameter fields to obtain velocity and water content distributions under gravity-driven flow for prescribed values of soil-moisture tension.
2. Solve the ADE with a total variation diminishing (TVD) scheme and with dispersivities and molecular diffusion coefficients set to zero, using STOMP for steady-state flow conditions with the selected hydraulic parameter fields.
3. Use flux plane output produced by STOMP to compute flux-averaged concentrations for different vertical transport distances.
4. Fit the ADE to the flux-averaged concentration results to estimate apparent dispersivity.

The ADE-based method is more convenient than moment-based methods but has the disadvantage of potentially introducing numerical dispersion into the results. The effects of numerical dispersion were reduced to the extent possible by using a TVD numerical scheme (Gupta et al. 1991) and setting both diffusion and dispersivity parameters to zero. For steady uni-directional flow conditions in a uniform material, and with constant grid spacing and Courant number $\equiv 1$, the numerical solution obtained using the TVD scheme should be strictly advective with a very sharp (step-function-type) front and negligible numerical dispersion. In practice, for non-uniform materials and with variable Courant number conditions, the numerical approximations of gradient operators in the ADE are expected to introduce some dispersive effects, but these are difficult to distinguish from heterogeneity-induced dispersion. Use of the TVD solution scheme effectively eliminates Peclet number constraints, but a strict Courant number limit ≤ 1 is still required.

2.3.1 STOMP Model Setup

Numerical simulations for the ADE-based estimation of dispersivity were performed with a 4-m by 4-m by 4-m model domain, discretized with uniform 0.05 m grid spacing in each direction, yielding 512,000 model grid blocks. It is assumed that waste packages will be placed relatively close together within the IDF pit, such that the distance between waste packages will be less than 4 m. Hydraulic parameter fields generated on this domain were used by Zhang (2010) in an earlier study on upscaling of hydraulic parameters. The domain size and discretization used with the particle-based approach, described previously, differ from those used for the ADE-based approach described here because the former used

IDF site-specific characterization data and a larger domain for which coarser discretization was needed. Except for the addition of solute transport, and specification of flux planes in the model, the model setup from Zhang (2010) was used as-is for consistency with the setup used for the previously published results.

Synthetic “Miller-similar” parameter fields described by Zhang (2010) were used (Figure 6). Miller-similar refers to geometrically similar porous media that have uniform porosity and similar particle and pore structures, but that vary in the mean sizes of particles and pores at different locations (Miller and Miller 1956; Rockhold et al. 1996). A Miller-similar porous media would have constant porosity (or θ_s), constant residual water content (θ_r), and constant van Genuchten (1980) model n parameter, but the saturated hydraulic conductivity (K_s) and van Genuchten model α parameters would be variable and related to each other at different locations by scaling factors.

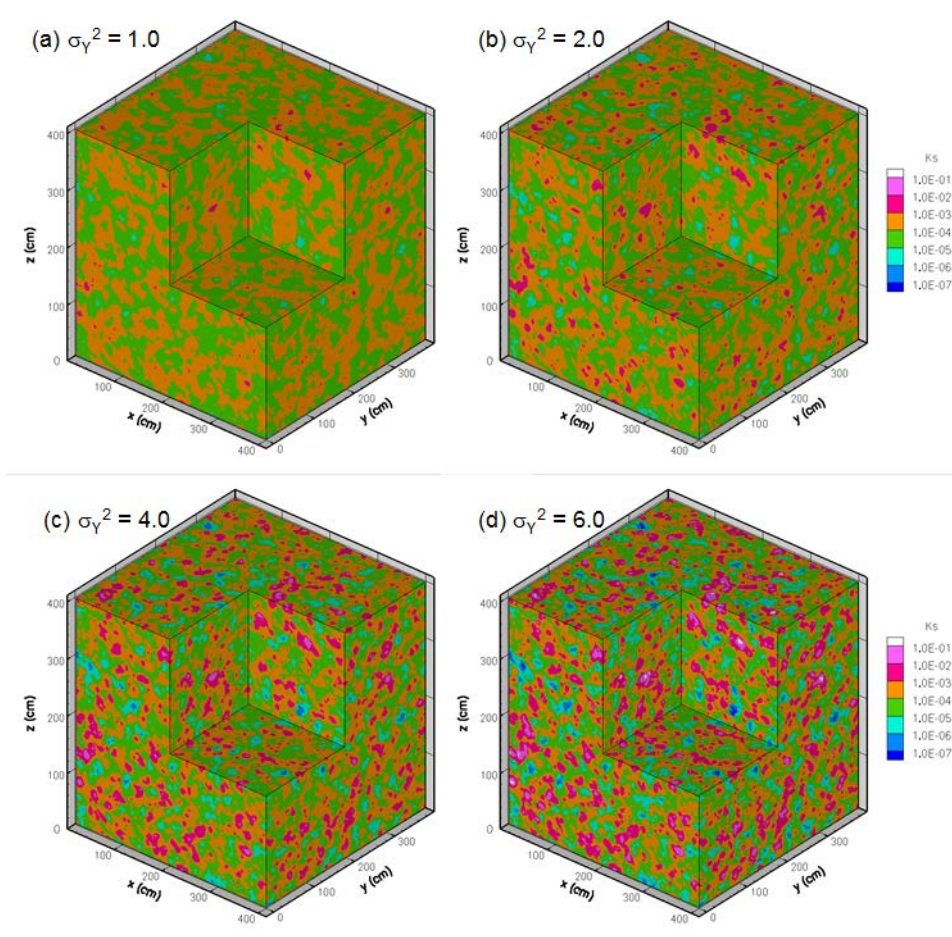


Figure 6. Miller-similar porous media with different levels of heterogeneity in $Y=\ln(K_s)$. The variance of $\ln(K_s)$ is denoted σ_Y^2 . The geometric mean of K_s for all fields is 1.0×10^{-2} cm/s (after Figure 1 of Zhang 2010).

Figure 6 shows examples of isotropic Miller-similar hydraulic conductivity fields used by Zhang (2010) with different levels of heterogeneity for $\ln(K_s)$. Although the synthetic, isotropic Miller-similar parameter fields do not resemble the strongly layered sediment profile depicted in Figure 2, or the anisotropic fields shown in Figure 5 that were conditioned on IDF site-specific data, there may be areas associated with the IDF where the sediments have similar characteristics. For example, at smaller scales

in the near-field environment surrounding waste packages, the sediments will likely be less structured and more homogeneous than seen in undisturbed regions, due to disturbance of structure and homogenization associated with excavation and backfilling. The results obtained with the Miller-similar synthetic soils are applicable to those areas.

The effective hydraulic properties of the Miller-similar porous media shown in Figure 6 are summarized in Table 2 of Zhang (2010). Figure 7 shows how the variance of (unsaturated) hydraulic conductivity changes with mean pressure head for these porous media with different levels of heterogeneity.

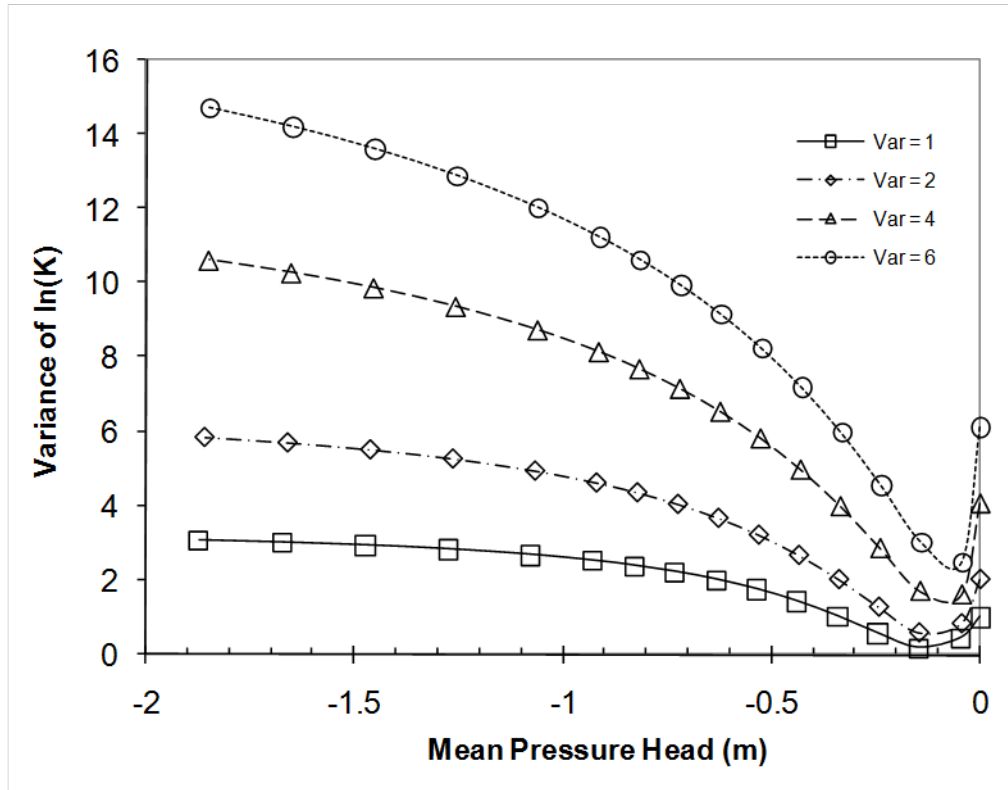


Figure 7. Variance of $\ln(K)$ as function of mean pressure head for the synthetic soils with different levels of heterogeneity. $\text{Var} = \sigma_Y^2$ and $Y = \ln(K_s)$ (after Figure 2 of Zhang 2010).

Using the generated synthetic soils, numerical experiments of gravity-driven flow were carried out under Dirichlet-type constant-head boundary conditions at both the top and bottom boundaries using STOMP. The lateral boundary conditions were specified as Neumann-type zero flux boundaries. The head values at the top and bottom boundaries were kept the same (i.e., at -0.5, -1.0, or -1.5 m of pressure head) for each simulation so gravity was the only driving force. These boundary conditions were used previously by Zhang (2010) in his upscaling studies. Both 3-D and 1-D simulations were performed. For the 1-D simulations, ten 1-D profiles were sampled from the 3-D fields and simulations were performed with each.

After steady state was achieved for each hydraulic parameter field, a uniform concentration of solute was specified at the upper boundary of the model domain for a 1-day period for $h = -0.5$ m, and for 10-day periods for $h = -1.0$ m and -1.5 m. Horizontal flux planes were specified in the model at 0.5-m

depth intervals from the 0.5 to 4.0 m depths. Aqueous (q_w) and solute (q_s) fluxes were output from STOMP for the flux planes and the flux-averaged concentrations were calculated as $C = q_s/q_w$.

2.3.2 Estimation of Dispensivity

The following analytical solution to the ADE was fit to the simulated breakthrough curves of flux – average concentration (Leij and van Genuchten 2002)

$$C_{step}(x,t) = \frac{C_0}{2} \left[\operatorname{erfc} \left(\frac{x - vt}{2(Dt)^{1/2}} \right) + \exp \left(\frac{vx}{D} \right) \operatorname{erfc} \left(\frac{x + vt}{2(Dt)^{1/2}} \right) \right] \quad (8)$$

where C_0 is the applied concentration, x is distance, v is pore-water velocity, t is time, D is the dispersion coefficient, and exp and $erfc$ are the exponential and complementary error functions, respectively. For solute input as a pulse from times t_1 to t_2 , the solution is

$$C(x,t) = C_{step}(x,t - t_1) - C_{step}(x,t - t_2) \quad (9)$$

The parameters D and v were fit to the flux-averaged concentration results. The dispersivity in the vertical direction was then calculated as $A_{zz} = D/v$.

3.0 Results and Discussion

This section is divided into two parts. The first part (Section 3.1) presents results obtained from the particle-based method of estimating dispersivity, based on hydraulic parameter fields conditioned on core data from characterization well 299-E17-21, and using information on spatial autocorrelation of physical properties from the Sisson and Lu site. The second part (Section 3.2) presents results obtained using the ADE-based method for synthetic, isotropic Miller-similar porous media.

3.1 Particle-Based Dispersivity Estimation

Five stochastic realizations of hydraulic parameter fields were generated. Simulations were performed for three of these realizations (e.g., Figure 5) and for three infiltration rates (0.5, 1.0, and 3.5 mm/yr) representative of natural groundwater recharge rates around the IDF (Fayer and Szecsody 2004). The average/standard deviation of water content for the three realizations combined are 0.073/0.041, 0.078/0.044, and 0.088/0.048 for recharge rates of 0.5, 1.0, and 3.5 mm/yr respectively. The average/standard deviation of soil moisture tension (in units of cm) for the three realizations combined are 416/195, 353/162, and 262/118 for recharge rates of 0.5, 1, and 3.5 mm/yr, respectively. Ideally, simulations would be performed with many more realizations of the hydraulic parameter fields to evaluate the ensemble average behavior of transport results (Khaleel et al. 2002). Ensemble average transport behavior for a large number of realizations could not be evaluated owing to schedule constraints, but this may be addressed in future efforts. Uncertainty analysis was also outside the scope of the current effort, so only three realizations were selected and used to generate the results reported here.

Figure 8 shows snapshots of particle clouds at different times for one realization and a recharge rate of 3.5 mm/yr. When all particles are viewed together as a cloud, they appear to be one relatively cohesive group moving together. However, Figure 9 shows the paths of nine particles from this simulation. When viewed individually, it is clear that any given particle may follow a very tortuous path. Although the mean flow direction is vertical, significant lateral diversions of the particles are evident. Results for the other two recharge rates (0.5 and 1 mm/yr) are similar, although the particle trajectories change to some extent. Calculated dispersivity values for all three recharge rates are shown in Figure 10.

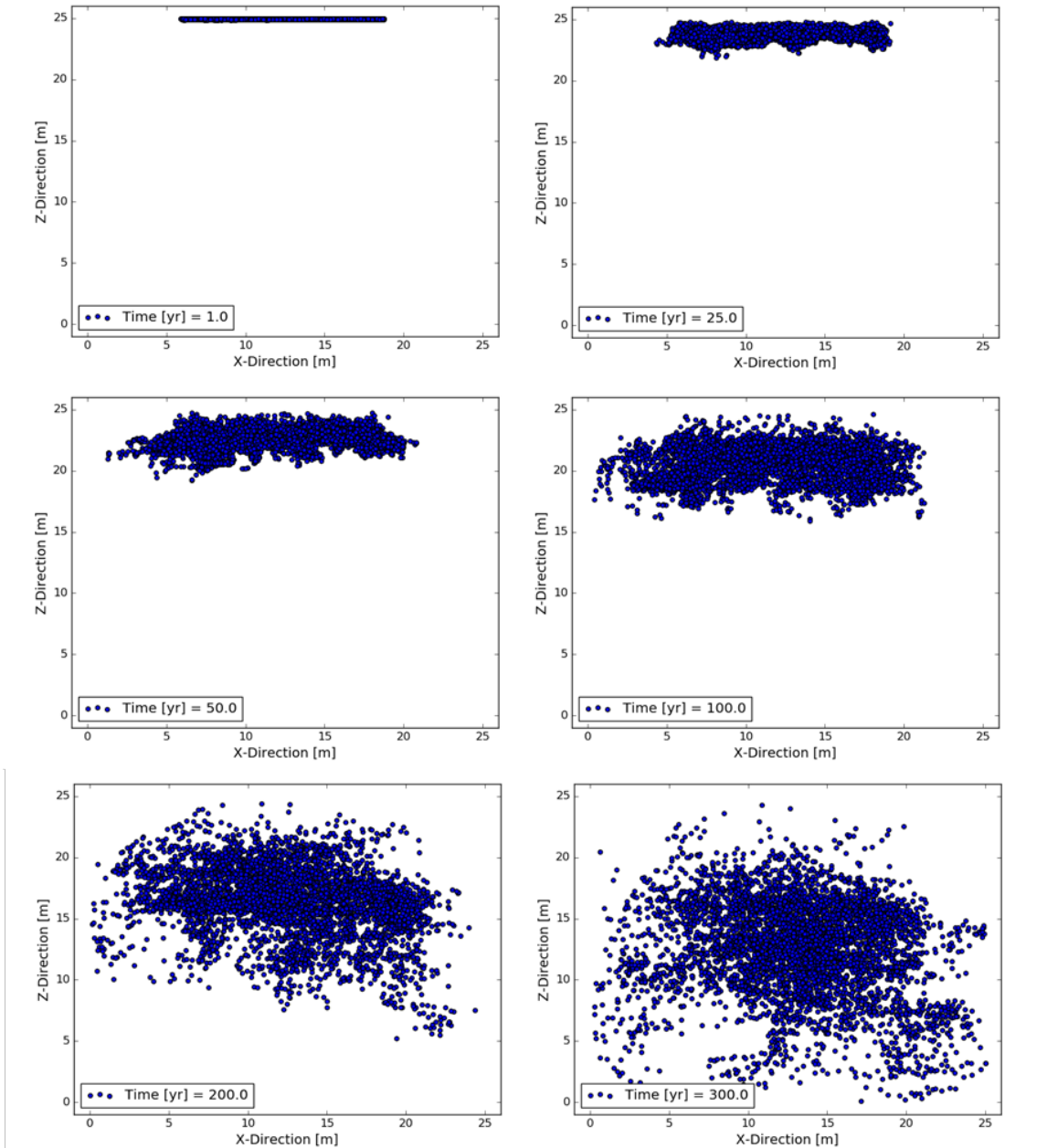


Figure 8. Snapshots of the locations of 5000 particles at different times for a flow field corresponding to hydraulic parameters for SGSIM realization 5 and a recharge rate of 3.5 mm/yr.

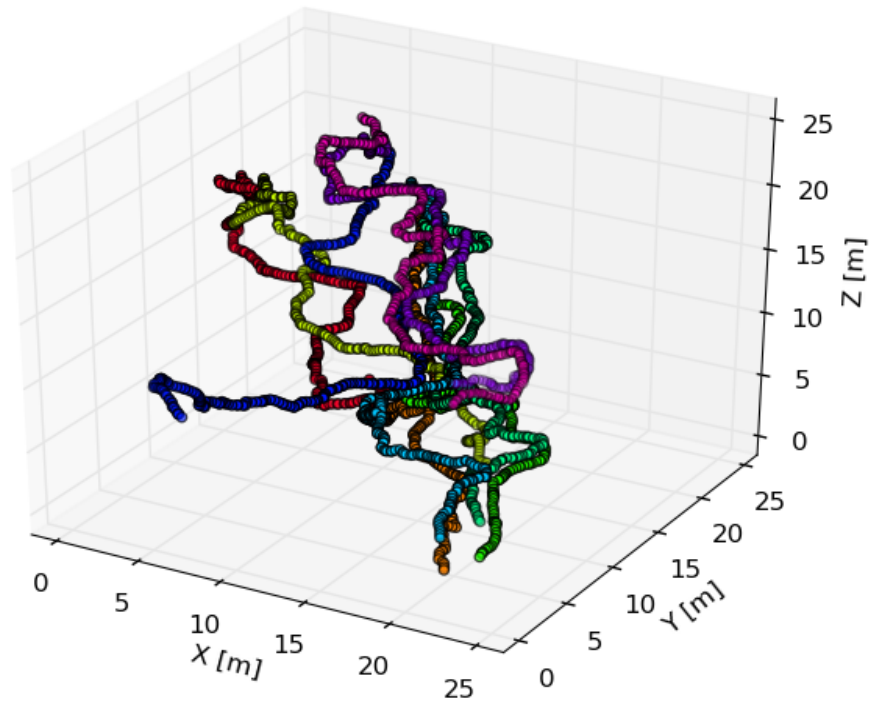


Figure 9. Paths of nine selected particles from the simulation that produced Figure 10.

Figure 10 shows the calculated apparent dispersivity values for the vertical direction calculated using Eq. (7) for the three stochastic realizations of hydraulic parameters, and three recharge rates. Dispersivities for all realizations and all recharge rates increase with increasing travel distance, with no obvious attainment of asymptotic (near constant) values. Although not obvious from Figure 10, the calculated dispersivity values decrease slightly for higher recharge rates, which correspond to slightly higher water contents or saturations. The three recharge rates that were evaluated are all very low, so the water contents are also very low and the effects of changes in water content or saturation on dispersion are less significant than they might be for a wider range of recharge rates. At shorter transport distances (<1.5 m) the dispersivity estimates from the particle-based method are consistent with those determined in earlier studies (Khaleel 2004; Rockhold et al. 2015a). It is noted that the ratio of dispersivity to vertical travel distance is on the order of 0.06-0.07, which is within the range of these ratios observed for saturated zone transport (Gelhar et al. 1992).

Spatial moment analysis has an advantage over temporal moments of allowing dispersivities to be estimated simultaneously for all principal directions. Dispersivity values calculated from Eq. (7), but also using σ_{xx}^2 and σ_{yy}^2 in addition to σ_{zz}^2 , are listed in Table 2 for stochastic realization number 5. Calculated dispersivities are reported for space-time scales in which >95% of the particles remained within the model domain, so reported travel distances are significantly shorter than the vertical extent of the model domain. Interestingly, the calculated dispersivities in the principal horizontal directions (XX and YY) are generally of the same order of magnitude as the vertical direction (ZZ).

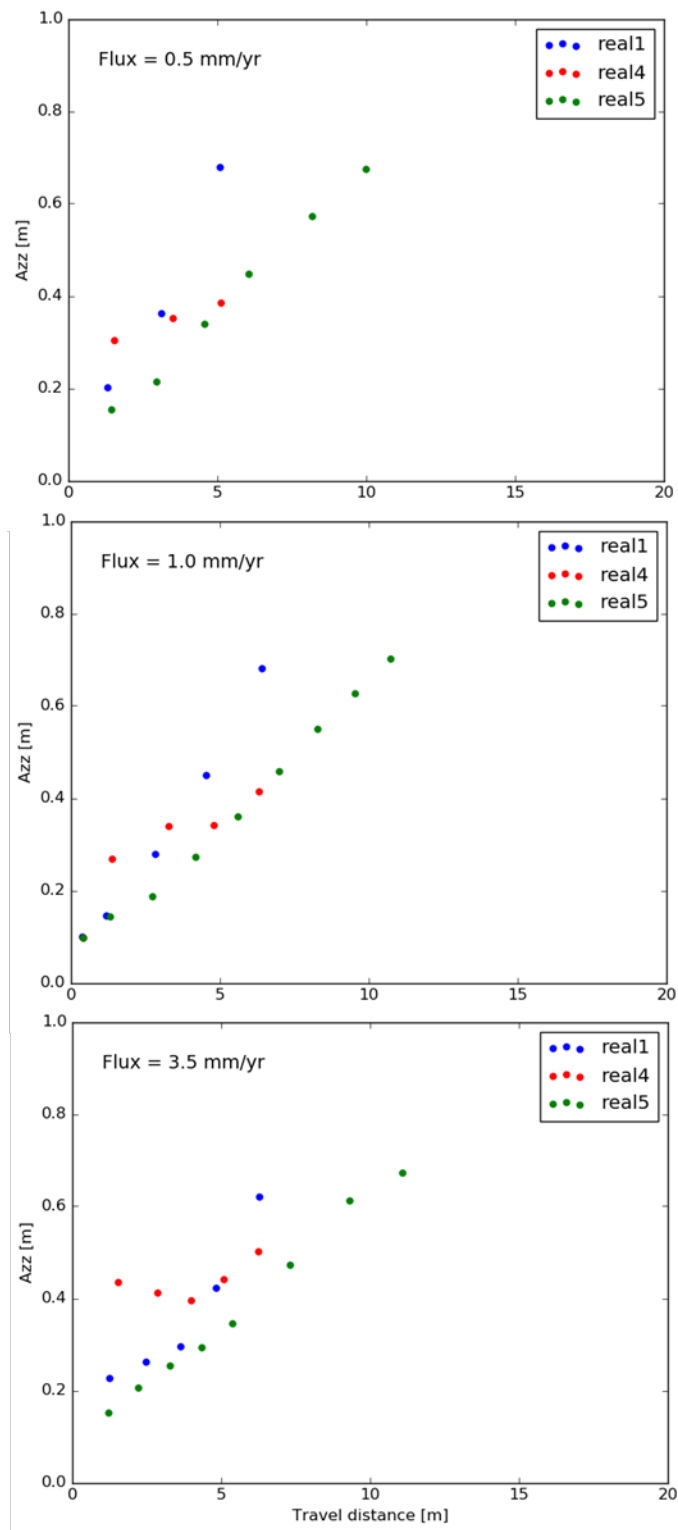


Figure 10. Apparent dispersivity in the vertical direction for three realizations of hydraulic parameters and three recharge rates.

Considering the pathlines shown in Figure 9, this result is not unexpected, but it runs counter to the rule-of-thumb, often used for transport modeling in saturated aquifer systems, of having transverse dispersivity be 1/10th the value of longitudinal dispersivity. Differences between the trends of A_{xx} and A_{yy} may be attributable to anisotropy in the X-Y plane.

Inspection of results indicates that particle dispersion normal to the principal flow direction may be influenced by the no-flow side boundaries of the model domain. This suggests that a larger domain, or smaller area for initial placement of particles, and/or periodic boundary conditions might be needed to eliminate or reduce boundary effects. These issues were discussed in some detail by Cirpka and Kitanidis (2002), who used periodic boundary conditions to minimize boundary effects. The fact that asymptotic behavior was not achieved for the vertical transport direction also suggests that a model domain with larger vertical extent should be evaluated.

Finally, it should be noted that in STOMP the dispersion coefficient is a second-order symmetric tensor. The longitudinal and transverse dispersivities are not assigned to any particular coordinate direction but the components of the hydrodynamic dispersion coefficient are computed for each principal flow direction using the directional components of the Darcy flux and both the longitudinal and transverse dispersivities (White and Oostrom, 2000). For vadose zone transport, it is apparent from the particle tracking results that the local flow directions can vary substantially even when the mean flow is in the vertical direction.

Table 2. Calculated apparent values of dispersivity in three directions for realization 5.

Recharge Rate (mm/yr)	Vertical Travel				
	Distance (m)	A_{xx} (m)	A_{yy} (m)	A_{zz} (m)	
0.5	1.44	1.67	0.01	0.15	
	2.98	1.43	0.17	0.21	
	4.57	1.07	0.39	0.34	
	6.08	0.98	0.53	0.45	
	8.18	0.83	0.90	0.57	
	10.01	0.61	1.08	0.67	
1.0	0.42	0.61	0.10	0.10	
	1.33	1.27	0.01	0.14	
	2.76	1.42	0.09	0.19	
	4.18	1.02	0.30	0.27	
	5.61	0.94	0.46	0.36	
	7.00	0.87	0.63	0.46	
	8.30	0.75	0.93	0.55	
	9.55	0.59	1.12	0.63	
10.73	0.49	1.12	0.70		
3.5	1.21	1.51	0.08	0.15	
	2.24	1.33	0.10	0.21	
	3.28	0.99	0.25	0.25	
	4.35	0.85	0.38	0.29	
	5.39	0.77	0.54	0.34	
	7.33	0.58	0.88	0.47	
	9.31	0.40	1.07	0.61	
	11.10	0.34	1.02	0.67	

3.2 ADE-Based Dispersivity Estimation

Figure 11 shows calculated dispersivity values versus travel distance for the four synthetic Miller-similar porous media, denoted V1.0 through V4.0, for both 1-D and 3-D simulations, and three different soil water pressure heads ($h = -0.5, -1.0, \text{ and } -1.5 \text{ m}$). For the 1-D scenario with the wettest soil condition ($h = -0.5 \text{ m}$, Figure 11.a.1), the estimated dispersivity is near zero (no more than 0.01 m). For the corresponding 3-D case (Figure 11.bb1), A_{zz} is slightly larger but no more than 0.07 m. As the soil becomes drier (Figure 11a2 and a3 for the 1-D cases; b2 and b3 for the 3-D cases), A_{zz} also becomes larger because the variance of $\ln(K)$ increases with decreasing wetness (or pressure head, see Figure 7). A_{zz} is nearly independent of travel distance for the 1-D cases, while increasing gradually for the 3-D cases.

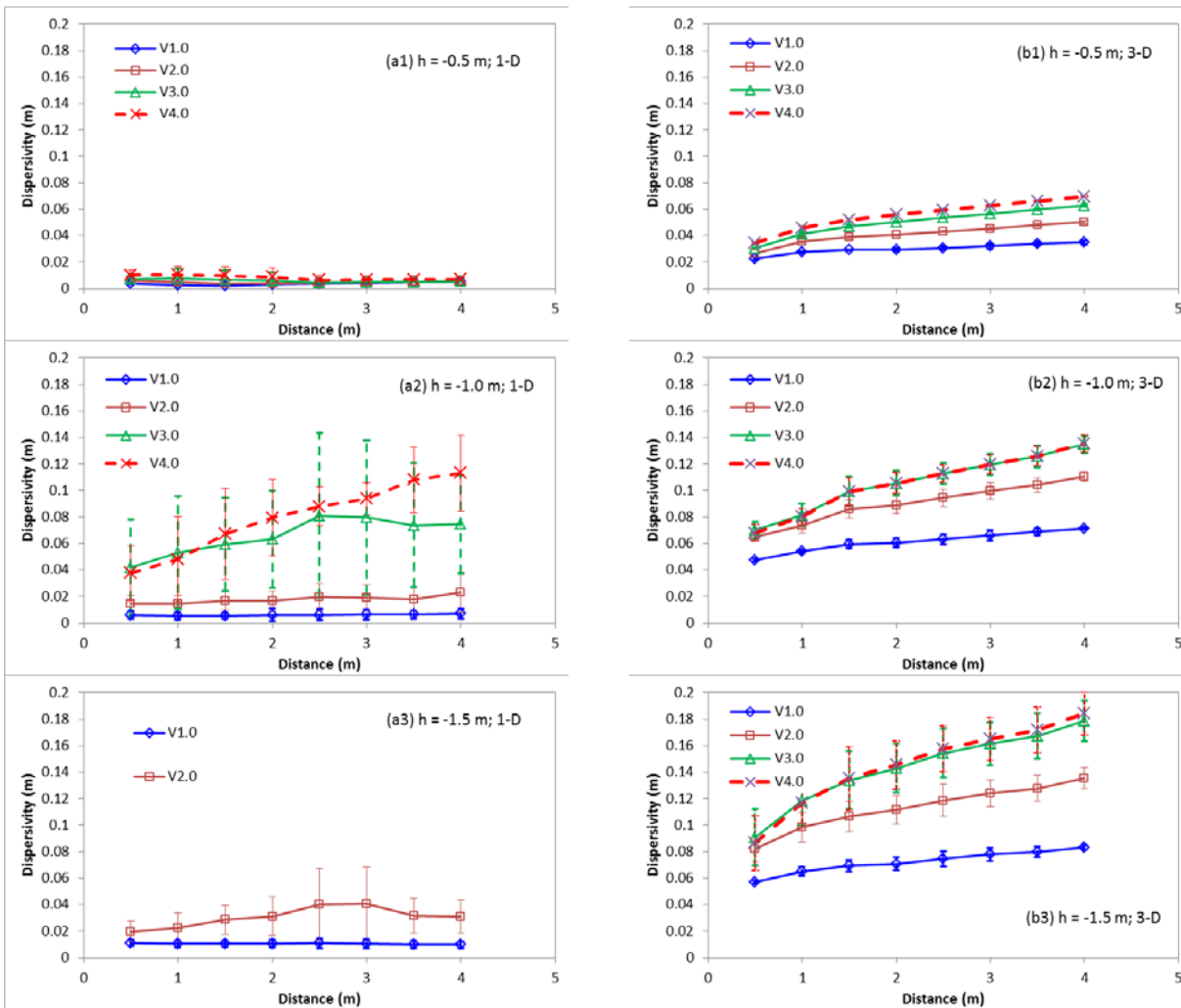


Figure 11. Solute longitudinal dispersivity (a) under 1-D heterogeneity and (b) 3-D heterogeneity conditions. The 1-D results were based on 10 simulations and the 3-D results were based on 3 simulations. For the 1-D, $h = -1.5 \text{ m}$ scenarios (plot a3, the breakthrough for V3.0 and V4.0 did not occur because the flow rates were too low). The vertical bars indicate one standard deviation.

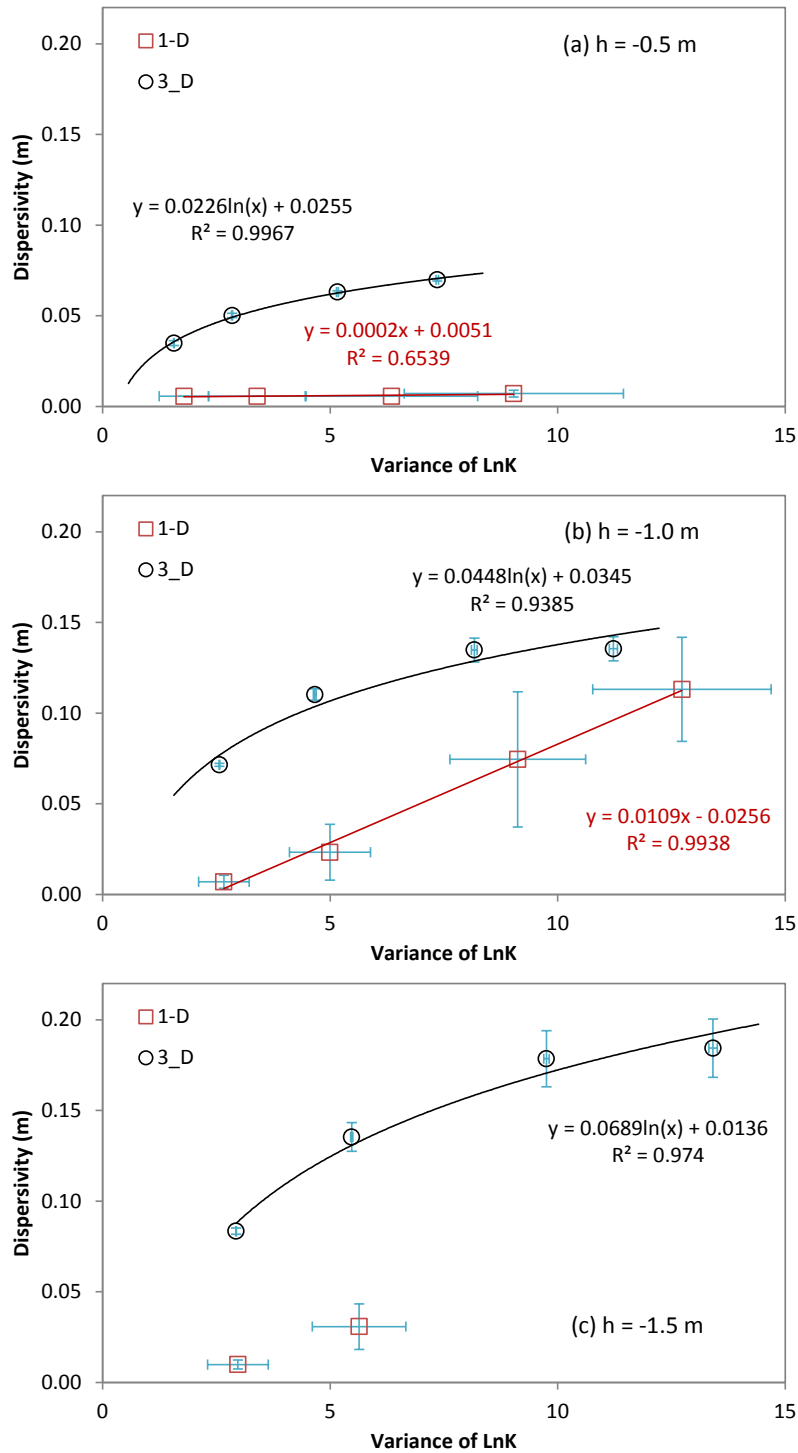


Figure 12. Impacts of soil spatial variability on solute longitudinal dispersivity at 4 m for 1-D and 3-D heterogeneity conditions. 1-D results based on 10 simulations and 3-D results were based on 3 simulations. For the 1-D, h = -1.5 m scenarios (plot c), solute breakthrough for V3.0 and V4.0 did not occur because the flow rates were too low. Symbols show average values and capped horizontal and vertical lines are one standard deviation of dispersivity and ln(K), respectively.

Note that Zhang et al. (2009; 2011) report average values of soil moisture tension measured at the 5 and 10 m depths under interim surface barriers covering the T and TY Tank Farms that range from 0.51 to 3.16 m. Therefore the tensions used for the simulations reported here are within the range of measured values for backfill sediments at Hanford under an infiltration barrier, which is the expected condition for waste packages in the IDF. However, additional simulations could be performed to evaluate dispersivity for these materials at higher tensions.

Figure 12 shows dispersivity at a 4 m transport distance versus the variance of $\ln(K)$. It appears that the relation is nearly linear for the 1-D cases and log-linear for the 3-D cases. For both the 1-D and 3-D cases, the slope increases as soils become drier (from $h = -0.5$ to $h = -1.5$ m). It also appears that use of 1-D transport calculations would significantly underestimate the longitudinal dispersion of solutes, compared to using 3-D calculations.

Given knowledge of the soil moisture tension regime, and the variance of $\ln(K)$, the 3-D results in Figure 11 and Figure 12 may be used to estimate dispersivity values for the near-field environment of the backfilled sediments surrounding waste packages at the IDF site. Ideally, more simulations would be performed to produce more robust estimates of ensemble mean values of dispersivity with error estimates. Use of a wider range of conditions (higher soil moisture tensions) would also be desirable.

4.0 Summary and Conclusions

The work described in this report was performed to evaluate alternative methods for estimating dispersivity for application to vadose zone transport modeling at the Hanford IDF site. Dispersivity estimates were derived using two methods: 1) a particle-based method with spatial moment analysis, and 2) an ADE-based method with calculation of dispersivity from flux-average concentrations determined for flux planes placed at different distances along the mean flow direction. The general findings are as follows:

- For any given distribution of vadose zone hydraulic parameters, apparent dispersivity increases with increasing space-time scales.
- For a fixed domain size, apparent dispersivity increases with increasing heterogeneity.
- Apparent dispersivity increases with decreasing water content, which is attributed to higher variance of unsaturated hydraulic conductivity at lower water content values.

For IDF site-specific transport calculations, the following recommendations are made:

- For the near-field environment of the backfill surrounding waste packages, results presented in Section 3.2, ADE-Based Dispersivity Estimation, may be used to select appropriate values of longitudinal dispersivity that depend on the expected range of soil moisture tension and the level of heterogeneity. Results suggest that longitudinal dispersivity values on the order of a few centimeters up to ~ 0.2 m may be appropriate for the near-field environment. For the shorter transport distances (~ 1 m), the ADE-based dispersivity estimates are similar to those determined experimentally for Hanford sediments by Rockhold et al. (2015a).
- For the sandy sediments of the far-field environment underlying the IDF, results presented in Section 3.1, Particle-Based Dispersivity Estimation, may be used to select approximate values of longitudinal

dispersivity. However, asymptotic dispersivity values were not reached over the limited vertical transport distances that were evaluated using the particle-based method. Considering uncertainties associated with the heterogeneity of the unsampled subsurface underlying the IDF site, the higher (more conservative) peak concentrations that are obtained using smaller values of dispersivity relative to larger values, and numerical dispersion, results suggest that longitudinal dispersivity values on the order of tens of centimeters up to ~ 1 m may be applicable to the sandy vadose zone sediments of the far-field environment. These estimates of dispersivity for the sandy sediments underlying the IDF are similar to those used in earlier IDF PAs (Khaleel 2004), but the methods and results reported here provide an alternative technical basis.

- For the gravelly sediments of the far-field environment underlying the IDF, dispersivity estimates from Khaleel (2004) or Rockhold et al. (2015b) may be used. Those estimates, which use alternative technical bases, differ by less than a factor of 1.5. Previous work by Khaleel and Relyea (2001) suggests that if the sediments underlying the IDF have hydraulic properties that are similar to those measured for sandy and gravelly sediment samples collected elsewhere at Hanford, the dispersivity of the gravelly sediment should be smaller than that of the sandy sediment owing to lower variance of unsaturated hydraulic conductivity. The unsaturated hydraulic conductivity estimates for the sandy and gravelly sediments reported by Rockhold et al. (2015b) are also supportive of the idea that the dispersivity of the gravelly sediments may be smaller than that of the sandy sediments. However, previous dispersivity estimates reported for gravelly sediments by Rockhold et al. (2015b) based on empirical correlation functions and grain size data were slightly larger than those estimated for the sandy sediments, owing to the more non-uniform grain size distributions for the gravelly sediments.
- It is suggested that PA calculations be performed to evaluate the sensitivity of model results to dispersivity estimates for both the sandy and gravelly sediments, as well as the near field (backfill) materials.

Dispersivity estimates for the IDF site are summarized in Table 3. The majority of the dispersivity calculations described herein represent mean transport in the vertical direction, which may be thought of as the longitudinal direction for transport through the vadose zone. Particle-tracking results show that significant lateral diversions occur under variably saturated conditions, even for steady mean vertical flow. Further analysis using results from particle-based methods would be required to provide additional insight or guidance on selection of transverse dispersivity values for application to vadose zone transport modeling. Khaleel (2004) and Rockhold et al. (2015b) both suggested that transverse dispersivity values be estimated as $1/10^{\text{th}}$ the value of the longitudinal dispersivity. This recommendation currently stands until additional numerical experiments are performed that provide further insights and more definitive results.

In conclusion, the results of this study demonstrate that the estimation of dispersivity for variably saturated porous media is not completely straightforward. Dispersion depends on many related factors including scale, heterogeneity, and water content or saturation, with the latter dependent on both porous media characteristics and flow rates (recharge rates). The sparse nature of characterization data at the Hanford Site, and highly heterogeneous nature of the subsurface, make it difficult to estimate physical and hydraulic properties at relevant scales with certainty. Additional high-resolution simulations, using stochastic realizations of hydraulic parameters, could be used to assess the uncertainty in flow and transport behavior for the IDF site resulting from the spatial variability and scale-dependence of physical,

hydraulic, and transport parameters. Particle tracking results from this study also indicate that larger spatial domains should be evaluated.

Table 3. Estimated longitudinal (A_{zz}) and transverse (A_{xx} , A_{yy}) dispersivity values for the IDF site.

Material	A_{zz} (m)	A_{xx} , A_{yy} (m)	Assumed Conditions
Backfill	0.15 [†]	0.1* A_{zz}	[†] $h = 1.5$ m
Sandy Sequence	0.7 [‡] – 2.0 [§]	0.1* A_{zz}	[‡] $q = 0.5 - 3.5$ mm/yr [§] $h = 1.0$ m, $\lambda = 0.3$ m
Gravelly Sequence	0.3 [§] – 0.43 [¶]	0.1* A_{zz}	[§] $h = 1.0$ m, $\lambda = 0.3$ m [¶] empirical correlation from grain size distribution metrics; $S = 0.25$

[†] This report (Figures 7, 11, and 12), assuming variance of $\ln(K_s) \approx 2$, variance of $\ln(K) \approx 6$. Parameter h is soil moisture tension.

[‡] This report (Figure 10 and Table 2). Parameter q is recharge rate.

[§] Khaleel (2004, Table 9). Parameter h and λ are soil moisture tension and vertical correlation length, respectively.

[¶] Rockhold et al. (2015, p.7.24). Parameter S is aqueous saturation.

5.0 Quality Assurance

This work was conducted with funding from Washington River Protection Solutions (WRPS) under contract 36437-161, ILAW Glass Testing for Disposal at IDF. The work was conducted as part of Pacific Northwest National Laboratory (PNNL) Project 66309, ILAW Glass Testing for Disposal at IDF.

All research and development (R&D) work at PNNL is performed in accordance with PNNL’s laboratory-level Quality Management Program, which is based on a graded application of NQA-1-2000, *Quality Assurance Requirements for Nuclear Facility Applications*, to R&D activities. In addition to the PNNL-wide quality assurance (QA) controls, the QA controls of the WRPS Waste Form Testing Program (WWFTP) QA program were also implemented for the work. The WWFTP QA program consists of the WWFTP Quality Assurance Plan (QA-WWFTP-001) and associated QA-NSLW-numbered procedures that provide detailed instructions for implementing NQA-1 requirements for R&D work. The WWFTP QA program is based on the requirements of NQA-1-2008, *Quality Assurance Requirements for Nuclear Facility Applications*, and NQA-1a-2009, *Addenda to ASME NQA-1-2008 Quality Assurance Requirements for Nuclear Facility Applications*, graded on the approach presented in NQA-1-2008, Part IV, Subpart 4.2, “Guidance on Graded Application of Quality Assurance (QA) for Nuclear-Related Research and Development.”

Performance of this work and preparation of this report were assigned the technology level “Applied Research” and were conducted in accordance with procedure QA-NSLW-1102, *Scientific Investigation for Applied Research*. All staff members contributing to the work have technical expertise in the subject matter and received QA training prior to performing quality-affecting work. The “Applied Research” technology level provides adequate controls to ensure that the activities were performed correctly. Use of both the PNNL-wide and WWFTP QA controls ensured that all client QA expectations were addressed in performing the work.

6.0 References

- Aris R. 1956. "On the Dispersion of a Solute Flowing Through a Tube." *Proc. R. Soc. London, Ser. A*, 235:67-78.
- ASME NQA-1-2000, *Quality Assurance Requirements for Nuclear Facility Applications*. American Society of Mechanical Engineers, New York.
- ASME NQA-1-2008, *Quality Assurance Requirements for Nuclear Facility Applications*. American Society of Mechanical Engineers, New York.
- ASME NQA-1a-2009, Addenda to ASME NQA-1-2008 Quality Assurance Requirements for Nuclear Facility Applications. American Society of Mechanical Engineers, New York.
- Bear J. 1972. *Dynamics of Fluids in Porous Media*. Dover Publications, Inc., New York
- Bjornstad BN. 2006. *On the Trail of the Ice Age Floods: A Geological Field Guide to the Mid-Columbia Basin*. Keokee Co. Publishing, Inc., Sandpoint, Idaho.
- Brooks RH and AT Corey. 1964. "Hydraulic Properties of Porous Media." *Hydrol. Pap. 3*, Colo. State Univ., Fort Collins.
- Carsel RF and RS Parrish. 1988. "Developing Joint Probability Distributions of Soil Water Retention Characteristics." *Water Resour. Res.* 24:755-769.
- Cirpka OA and PK Kitanidis. 2002. "Numerical Evaluation of Solute Dispersion and Dilution in Unsaturated Heterogeneous Media." *Water Resour. Res.* 38(11):1220. doi:10.1029/2001WR001262
- Dagan G. 1984. "Solute Transport in Heterogeneous Porous Formations." *J. Fluid Mech.* 145:151-177.
- Dagan G. 1989. *Flow and Transport in Porous Formations*. Springer-Verlag, Berlin.
- Deutsch CV and AG Journel. 1998. *GSLIB – Geostatistical Software Library and User's Guide*, 2nd Ed., Oxford University Press, New York.
- Fayer MJ, RE Lewis, RE Engleman, Al Pearson, CJ Murray, JL Smoot, PR Randall, WH Wegener, and AH Lu. 1995. *Reevaluation of a Subsurface Injection Experiment for Testing Flow and Transport Models*. PNL-10860, Pacific Northwest National Laboratory, Richland, Washington.
- Fayer MJ and JE Szecsody. 2004. *Recharge Data Package for the 2005 Integrated Disposal Facility Performance Assessment*. PNNL-14744. Pacific Northwest National Laboratory, Richland, Washington.
- Freyberg DL. 1986. "A Natural Gradient Experiment on Solute Transport in a Sand Aquifer. 2. Spatial Moments and Advection and Dispersion of Nonreactive Tracers." *Water Resour. Res.* 22(13):2031-2046.
- Gardner WR. 1958. "Some Steady-State Solutions of the Unsaturated Moisture Flow Equation with Application to Evaporation from a Water Table." *Soil Sci.* 85:228-232.

- Gelhar LW. 1993. *Stochastic Subsurface Hydrology*. Prentice-Hall, Inc.
- Gelhar LW and CL Axness. 1983. "Three-Dimensional Stochastic Analysis of Macrodispersion in Aquifers." *Water Resour. Res.* 19(1):161-180.
- Gelhar LW, MA Celia, and D McLaughlin. 1994. *Modeling Field Scale Unsaturated Flow and Transport Processes*. NUREG/CR-5965, U.S. Nuclear Regulatory Commission, Washington, D.C.
- Gupta AD, LW Lake, GA Pope, K Sefhernoori, and MJ King. 1991. "High-Resolution Monotonic Schemes for Reservoir Fluid Flow Simulation." *In Situ* 15(3):289-317.
- Güven O, FJ Molz, and JG Melville. 1984. "An Analysis of Dispersion in a Stratified Aquifer." *Water Resour. Res.* 20(10):1337-1354.
- Harter T and D Zhang. 1999. "Water Flow and Solute Spreading in Heterogeneous Soils with Spatially Variable Water Content." *Water Resour. Res.* 35(2):415-426.
- Jury WA and K Roth. 1990. *Transfer Functions and Solute Movement Through Soil*. Birkhäuser Verlag Basel.
- Khaleel R, TE Jones, AJ Knepp, FM Mann, DA Myers, PM Rogers, RJ Serne, and MI Wood. 2000. *Modeling Data Package for S-SX Field Investigation report (FIR)*. RPP-6296, Rev. 0, CH2M Hill Hanford Group, Inc. Richland, Washington.
- Khaleel R, and JF Relyea. 2001. "Variability of Gardner's α for Coarse-Textured Sediments." *Water Resour. Res.* 37:1567-1575.
- Khaleel R, T -C J Yeh, and Z Lu. 2002. "Upscaled Flow and Transport Properties for Heterogeneous Unsaturated Media." *Water Resour. Res.* 38, No. 5, 1053, doi:10.1029/2000WR000072.
- Khaleel R. 2004. *Far-Field Hydrology Data Package for Integrated Disposal Facility Performance Assessment*. RPP-20621, Rev. 0, CH2M Hill Hanford Group, Inc., Richland, Washington.
- Last GV and TG Caldwell. 2001. *Core Sampling in Support of the Vadose Zone Transport Field Study*. PNNL-13454, Pacific Northwest National Laboratory, Richland, Washington.
- Leij FJ and MT van Genuchten. 2002. "Solute Transport." In *Soil Physics Companion*, AW Warrick (ed.), pp. 189-248. CRC Press, Boca Raton.
- Mantoglou A and LW Gelhar. 1985. *Large-Scale Models of Transient Unsaturated Flow and Contaminant Transport Using Stochastic Methods*. Report 299, Parsons Lab, Massachusetts Institute of Technology, Cambridge, Massachusetts.
- Meyer PD, ML Rockhold, and GW Gee. 1997. *Uncertainty Analyses of Infiltration and Subsurface Flow and Transport for SDMP Sites*. NUREG/CR-6565, PNNL-11705, Pacific Northwest National Laboratory, Richland, Washington.
- Miller EE and RD Miller. 1956. "Physical Theory for Capillary Flow Phenomena." *J. Appl. Phys.* 27:324-332.

Mualem Y. 1976. "A New Model for Predicting the Hydraulic Conductivity of Unsaturated Porous Media." *Water Resour. Res.* 12:513-522.

Nützmann G, S Maciejewski, and K Joswig. 2002. "Estimation of Water Saturation Dependence in Unsaturated Porous Media: Experiments and Modeling Analysis." *Adv. Water Resour.* 25:565-576.

Padilla IY, T-CJ Yeh, and MH Conklin. 1999. "The Effect of Water Content on Solute Transport in Unsaturated Porous Media." *Water Resour. Res.* 35(11):3303-3313.

Pollock DW. 1988. "Semianalytical Computation of Pathlines for Finite-Difference Models." *Ground Water* 26(6):743-750.

Polmann DJ. 1990. "Application of Stochastic Methods to Transient Flow and Transport in Heterogeneous Unsaturated Soils." PhD, Massachusetts Institute of Technology, Cambridge, Massachusetts.

Porro I, PJ Wierenga, and RG Hills. 1993. "Solute Transport Through Uniform and Layered Soil Columns." *Water Resour. Res.* 29(4):1321-1330.

Reidel SP. 2005. *Geologic Data Package for 2005 Integrated Disposal Facility Waste Performance Assessment*. PNNL-14586, Pacific Northwest National Laboratory, Richland, Washington.

Reidel SP and KR Fecht. 2005. *Geology of the Integrated Disposal Facility Trench*. PNNL-15237, Pacific Northwest National Laboratory, Richland, Washington.

Rockhold ML, RE Rossi, and RG Hills. 1996. "Application of Similar Media Scaling and Conditional Simulation for Modeling Water Flow and Tracer Transport at the Las Cruces Trench Site." *Water Resour. Res.* 32(3):595-609.

Rockhold ML. 1999. "Parameterizing Flow and Transport Models for Field-Scale Applications in Heterogeneous, Unsaturated Soils." In DL Corwin, K Loague, and TR Ellsworth (eds.), *Assessment of Non-Point Source Pollution in the Vadose Zone*. Geophysical Monograph 108, American Geophysical Union, Washington, D.C.

Rockhold ML, TW Wietsma, M Ostrom, AH Al-Shakarji, J Thomle, and DJ Swanberg. 2015a. *Effects of Grain-Size Distribution and Water Saturation on Solute Dispersion*. PNNL-24978, RPT-IGTP-008, Pacific Northwest National Laboratory, Richland, Washington.

Rockhold ML, ZF Zhang, PD Meyer, and JN Thomle. 2015b. *Physical, Hydraulic, and Transport Properties of Sediments and Engineered Materials Associated with Hanford Immobilized Low-Activity Waste*. PNNL-23711, RPT-IGTP-004, Rev. 0, Pacific Northwest National Laboratory, Richland, Washington.

Russo D. 1988. "Determining Soil Hydraulic Properties by Parameter Estimation: On the Selection of a Model for the Hydraulic Properties." *Water Resour. Res.* 24:453-459.

Russo D. 1993. "Stochastic Modeling of Macrodispersion for Solute Transport in a Heterogeneous Unsaturated Porous Formation." *Water Resour. Res.* 29:383-397.

- Russo D. 1998. "Stochastic Analysis of Flow and Transport in Unsaturated Heterogeneous Porous Formations: Effects of Variability in Water Saturation." *Water Resour. Res.* 34(4):569-581.
- Russo D. 2003. "Block-Effective Macrodispersion in Variably Saturated Heterogeneous Formations." *Water Resour. Res.* 39(12):1374. doi:10.1029/2003WR002724
- Schaap MG, PJ Shouse, and PD Meyer. 2003. *Laboratory Measurements of the Unsaturated Hydraulic Properties at the Vadose Zone Transport Field Study Site*. PNNL-14284, Pacific Northwest National Laboratory, Richland, Washington.
- Scheibe T and S Yabusaki. 1998. "Scaling of Flow and Transport Behavior in Heterogeneous Groundwater Systems." *Adv. Water Resour.* 22(3):223-238.
- Sisson JB and A Lu. 1984. *Field Calibration of Computer Models for Application to Buried Liquid Discharges: A Status Report*. RHO-ST-46 P, Rockwell Hanford Operations, Richland, Washington.
- van Genuchten MT. 1980. "A Closed-Form Equation for Predicting the Hydraulic Conductivity of Unsaturated Soils." *Soil Sci. Soc. America J.* 44:892-898.
- Ward AL, ME Conrad, WD Daily, JB Fink, VL Freedman, GW Gee, GM Hoverston, MJ Keller, EL Majer, CJ Murray, MD White, SB Yabusaki, and ZF Zhang. 2006. *Vadose Zone Transport Study Summary Report*. PNNL-15443, Pacific Northwest National Laboratory, Richland, Washington.
- Ward AL and ZF Zhang. 2007. "Effective Hydraulic Properties Determined from Transient Unsaturated Flow in Anisotropic Soils." *Vadose Zone J.* 6(4):913. doi:10.2136/vzj2006.0174
- Western AW and G Blöschl. 1999. "On the Spatial Scaling of Soil Moisture." *J. Hydrol.* 217:203-224.
- White MD, D Appriou, DH Bacon, Y Fang, VL Freedman, ML Rockhold, CM Ruprecht, GD Tartakovsky, SK White, and ZF Zhang. 2015. *STOMP/eSTOMP User Guide*. PNNL-SA-108766, Pacific Northwest National Laboratory, Richland, Washington. Accessed on October 29, 2015 at http://stomp.pnnl.gov/user_guide/STOMP_guide.stm.
- White MD and M Oostrom. 2000. *STOMP Subsurface Transport over Multiple Phases Version 2.0 Theory Guide*. PNNL-12030, Pacific Northwest National Laboratory, Richland, Washington.
- Yang J, R Zhang, J Wu, and MB Allen. 1996. "An Analytical Solution of Macrodispersivity for Adsorbing Solute Transport in Unsaturated Soils." *Water Resour. Res.* 32(2):355-362.
- Zhang D, TC Wallstrom, and CL Winter. 1998. "Stochastic Analysis of Steady-State Flow in Heterogeneous Media: Comparison of the Brooks-Corey and Gardner-Russo Models." *Water Resour. Res.* 34(6):1437-1449.
- Zhang ZF. 2010. "Effective Hydraulic Conductivity of Unsaturated Isotropic Soils with Multidimensional Heterogeneity," *Soil Sci. Soc. America J.* 74(3):734. doi:10.2136/sssaj2009.0405

Zhang ZF and R Khaleel. 2010. "Simulating Field-Scale Moisture Flow Using a Combined Power-Averaging and Tensorial Connectivity-Tortuosity Approach." *Water Resour. Res.* 46(9). doi:10.1029/2009wr008595

Zhang ZF, CE Strickland, JG Field, and DL Parker. 2009. *T Tank Farm Interim Surface Barrier Demonstration – Vadose Zone Monitoring FY08 Report*. PNNL-18083, Pacific Northwest National Laboratory, Richland, Washington.

Zhang ZF, CE Strickland, JG Field, and DL Parker. 2011. *T-TY Tank Farm Interim Surface Barrier Demonstration – Vadose Zone Monitoring FY10 Report*. PNNL-20144, Pacific Northwest National Laboratory, Richland, Washington.

Zhang ZF, AL Ward, and GW Gee. 2003. "A Tensorial Connectivity-Tortuosity Concept to Describe the Unsaturated Hydraulic Properties of Anisotropic Soils." *Vadose Zone J.* 2:313-321.

Distribution

**No. of
Copies**

Washington River Protection Solutions
DJ Swanberg
WRPS Documents – TOCVND@rl.gov

**No. of
Copies**

Pacific Northwest National Laboratory
DH Bacon
Y-J Bott
MJ Fayer
VL Freedman
ML Rockhold
ZF Zhang

Project File
Information Release (pdf)

*All distribution will be made electronically.



Pacific Northwest
NATIONAL LABORATORY

*Proudly Operated by **Battelle** Since 1965*

902 Battelle Boulevard
P.O. Box 999
Richland, WA 99352
1-888-375-PNNL (7665)

U.S. DEPARTMENT OF
ENERGY

www.pnnl.gov